Ferritin and its Biomedicine Applications

Laurel Gregory, Chloe Santiago*, Daisy Lindsey*

Department of Drug Quality Control and Pharmacovigilance, Ministry of Education, China Pharmaceutical University, Nanjing 210009, China

Review Article

*For Correspondence:

Chloe Santiago, Department of Drug Quality Control and Pharmacovigilance, Ministry of Education, China Pharmaceutical University, Nanjing 210009, China

Email: santiago.chloe@gmail.cn

Daisy Lindsey, Department of Drug Quality Control and Pharmacovigilance, Ministry of Education, China Pharmaceutical University, Nanjing 210009, China

**Email:** lindsey.daisy@gmail.cn

ABSTRACT

Ferritin with Nano-caged structure is a widely existing protein in the biological world that regulates iron metabolism in organisms. It is characterized by uniform size, good biocompatibility, good pH/temperature stability, reversible self-assembly, and adjustable functionalization, which shows ideal potential for practical applications. In this reviews, we focus on the unique structure of ferritin, the relative position of the loaded cargo, and the important impact of this position on its applications, including biosynthesis, bioimaging, disease treatment, etc. Finally, the prospects of ferritin in biomedicine are also discussed.

INTRODUCTION

Ferritin, the major iron storage protein in the body, is widely found in eukaryotes and prokaryotes [1]. It maintains the dynamic balance of iron storage and release in the life process [2]. Recently, in additional to regulating the iron metabolism, the level and structure of ferritin also shows close association with some diseases, such as neurodegenerative diseases [3-5], hereditary ferritinopathy, symptomatic knee osteoarthritis, iron deficiency anemia, Corona Virus disease 2019 (COVID-19), and immune-related pancytopenia [6-10]. For example, the brain diseases may be involved in the imbalance of ferritin subunits and its interaction with copper-containing Metallothionein 2-

subtype (MT2), which will lead to the release of toxic metal ion (such as Fe^{2+} and Cu^+) and then neuronal disorders [11]. As an endogenous protein, ferritin has good biocompatibility and biodegradability. The whole structure of ferritin is composed of multi-subunit, which can be self-assembled reversibly with surface porous structure and uniform size. It supplies a protein shell with a cavity to reversibly load and release cargoes. Moreover, ferritin has abundant amino acid residues on its inner/outer surface, which provides the active sites for chemical conjugation and biological recognition. Thus, ferritin has been extensively investigated in fields of dye delivery platform, regulation and secretion of ferritin, diagnosis and therapy of diseases, regenerative medicine, bioimaging, and biomimetic synthesis in recent years [12-26]. This review will briefly introduce the structure and superfamily function of ferritin, elaborates on the relative position of cargo-ferritin, and summarizes the application of ferritin in biomedicine and biotechnology in recent years (Figure 1).

Figure 1. Schematic illustration of ferritin-based multi-module platform in biomedicine. The whole structure is an alchemy furnace. The left arm represents different cargo molecules, i.e., the protein complex, and the right arm represents the final forms after ferritin modification. Three legs represent the relative positions of ferritin and cargo molecules: From left to right, they are cargo-embedded, double-interface-modified, and cargo-affixed ferritins, respectively. The structure information of protein shell is taken from RCSB (PDB code 6JPS) and processed by PyMOL software.
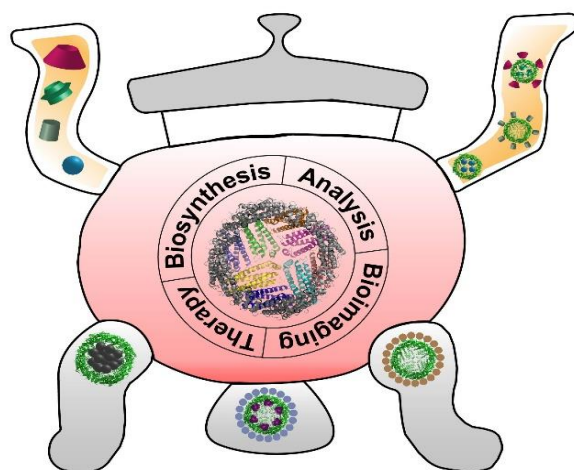

Structure and superfamily of ferritin

Structure of ferritin: In general, holo-ferritin is composed of a protein shell, called Apo ferritin, and a hydrated ferric oxide mineral core, i.e., ferrihydrite. The protein cavity of ferritin can store ca. 4500 ferric ions, which is 200 times that of hemoglobin. The subunits constituting the apoferritin are usually divided into heavy chain subunits (H subunits) and light chain subunits (L subunits). A few ferritins contain the third subunits, i.e., medium chain subunits (M subunits). The subunit sequence of the ferritin having been found is conserved and the relative mass of the subunits is equivalent, with the molecular weights of the H, M and L subunits of 22.8 kDa, 21.2 kDa and 20.0 kDa, respectively [27]. Different subunits form helical bundles with a certain spatial structure through five α-helices (A, B, C, D, and short E α-helix) and four flexible chains (A-B, B-C, C-D, D-E flexible chain). Among them, B-C is the longest one.

Ferritin is formed by 24 subunits with a 4-3-2 symmetric spherical structure, that is, a structure with 12 two-fold axis channels, 8 hydrophilic three-fold axis channels and 6 hydrophobic four-fold axis channels (Figures 2A-2C). These subunits form a nanocage structure, of which the outer diameter is 12 nm, inner diameter is 8 nm and

protein thickness is 2 nm. Besides classical ferritin with 24 subunits, there are ferritin superfamily with 12 subunits or monomeric protein, such as DNA binding proteins (Dps) from starved cells and archaeoferritin [28-31]. The assembly of ferritin is through Subunit-Subunit Interaction (SSIs), first the formation of a dimer by two single subunit, then a tetramer and a hexamer, and finally a complete protein cage [32]. By means of Small Angle X-ray Scattering (SAXS), High-Speed Atomic Force Microscopy (HS-AFM), and Molecular Dynamics (MD) simulation, it is found that subunit-subunit interaction among monomers and dimers play a key role in the reversible reassembly process of ferritin, especially head-body interfaces in dimeric interfaces [33-35].

Figure 2. Schematic diagram of channels on the surface of ferritin. (A) The two-fold axis channels, (B) The three-fold axis channels, (C) The four-fold axis channels of ferritin. The structure information is taken from RCSB (PDB code 6JPS) and processed by PyMOL.
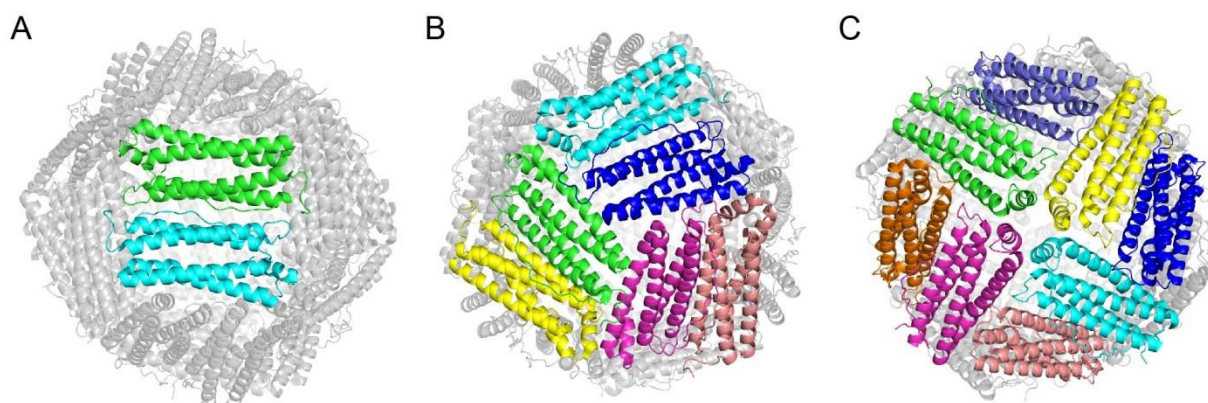
When the concentration of free iron increases in the body, ferritin will start up the nucleation process to play its role in iron storage and detoxification. In the ferritin nucleation process, the ferrous ions (Fe^{2+}) enter the ferroxidase center of H subunits through the hydrophilic three-fold channels and are oxidized to ferric irons (Fe^{3+}), followed by the hydrolysis and mineralization of ferric ions in the cavity of ferritin to form hydrated iron oxide-ferrihydrite. H subunits and L subunits play different roles in ferritin nucleation process. There is a di-nuclear Ferroxidase Center (FC) on each H subunit that could catalyze the oxidation of ferrous ions to ferric ions, but this center is absent on L subunits and replaced by specific amino acid residues with the function of binding metal ions and promotes the oxidation and mineralization of ferrous ions. Although lack of FC on the L subunit results in its ferroxidase being inactive, the L subunits of ferritin can facilitate iron turnover at FC site and promote the mineralization of ferric ions [36]. In the L subunit-rich ferritins or at high iron ion concentrations, the L subunits can mineralize iron ions on the surface of preformed ferrihydrite to form a larger core, thereby reducing the redox pressure at the FC and reducing the risk of free radical formation. This is consistent with the functions of different tissues in organisms. H-rich ferritins in heart and brain are helpful to avoid the toxicity of Fe^{2+} and L-rich ferritins in spleen and liver is helpful to enhance the storage of iron ions. According to the reaction kinetics and mechanism of self-assembly of H/L heteropolymeric ferritin by Fluorescence Resonance Energy Transfer (FRET) mechanism, it is found that the presence of H/L heterodimer was the basic condition for self-assembly of ferritin and the H/L heterodimer is easier to form than H/H or L/L homodimer [37].

Most of the iron oxide nanoparticles within natural ferritin are in the form of metastable ferrihydrite [38]. To understand the core of ferritin in different organs, Narayanan, et al. used *in situ* Graphene Liquid Cell-Transmission Electron Microscopy (GLC-TEM), Scanning Transmission Electron Microscopy (STEM), and Selected Area Electron

Diffraction (SAED) to analyse the differences in the morphology, composition and formation process of mineral cores between Human Heart Ferritin (HuHF) and Human Spleen Ferritin (HuSF) [39]. It is found that labile ferrihydrite is the main phases in hydrated HuSF and HuHF, while hematite (α-Fe_2O_3) is the main phase in non-hydrated HuSF and HuHF. Some techniques, such as electron energy loss spectroscopy, cryo-STEM, X-ray energy dispersive spectroscopy, and aberration-corrected TEMs, could also be used to explore biomineralization of iron oxide cores, so that the combination, nucleation, growth of cores in ferritin will be described more thoroughly [40,41].

## LITERATURE REVIEW

Superfamily of ferritin

As an iron storage protein, ferritin is ubiquitous in biological communities. Among ferritins investigated, they can be divided into eukaryotic ferritins (like animal ferritins and plant ferritins), bacterial ferritins, and archaeal ferritins, etc (Figure 3).

Animal ferritin is a classical protein molecule with a mass of about 500 kDa. Each ferritin molecule consists of 24 subunits to form a regular octahedron, of which each subunit is composed of 200 amino acids (Figure 3A). Natural animal ferritin is a heteropolymer composed of two different subunits, L-subunit and H-subunit. Both of them are rich in amino acid residues, which can be used for chemical or genetic modification. Different from animal ferritin, plant ferritin (phytoferritin) has only H subunits composed of H-1 and H-2 and has an exceptional Extension Peptide (EP) at N terminus of each subunit (Figure 3B). In different plants, the ratio of H-1 and H-2 is variant to regulate the movement of iron into and out of ferritin [42]. Moreover, phytoferritin has exceptional thermal stability, which means that the internal cargos will not be easily lost and invalid using phytoferritin as the carrier. Another difference from animal ferritin is the high phosphorus/iron ratio of plant ferritin, which not only makes phytoferritin a source of iron or phosphorus, but also increases its oxidative stress capacity at low iron loading. For example, phytoferritin can protect the loaded DNA at the low ferrous iron concentration (<48 Fe^{2+} per protein shell) [43,44].

Bacteria also contain some ferritins with a special structure, such as Bacterioferritins (BFRs), Dps, and Encapsulin Ferritins (EncFtns). Unlike classical ferritins (Figure 3C), BFRs contain twelve b-type heme cofactors at two-fold pores, which may be involved in the electron transfer during iron oxidation/mineralization process and enhanced protein stability and iron release procedure of BFRs (Figure 3D) [45-47]. Dps is a 12-mer ferritin, which can protect DNA from oxidative damage and is related to the survival and virulence of bacteria (Figure 3E) [48]. EncFtn is the largest ferritin-like protein in ferritin superfamily, which is consisted by 60 subunits, 180 subunits or 240 subunits. The big cavity and/or channels of EncFtn allow residency and entry of other enzymes or ferritins (Figure 3F) [49,50]. Archaeoferritin is a protein coming from archaea, a protein monomer with ferroxidase activity in the absence of iron (Figure 3G). It is more widely used in the biomedical and nanotechnology filed due to the properties of self-assembly under mild conditions and large-sized pores on the surface. Besides, the symmetry of archaeoferritin is also different from the classical 4-3-2 symmetry. For instance, the ferritin derived from Archaeon *Archaeoglobus fulgidus* consists of 24 subunits, presenting 2-3 symmetry.

Figure 3. Representative diagram of the quaternary structure (the upper part of each Figure) and its corresponding subunits (the lower part of each Figure) of the ferritin superfamily. (A) Human heavy chain ferritin (PDB ID 2FHA). (B) Phytoferritin from glycine max (PDB ID 3A68), its subunits have an extension peptide (red) at N terminus. (C) Bacterial ferritin (PDB ID 4XGS), (D) bacterioferritin (PDB ID 3E1O) with a heme group between two-fold channels (red), and (E) Dps (PDB ID 6GCM) with a different helix in BC-loop (red) from *Escherichia coli* K-12. (F) Encapsulin

shell protein EncA with T=1 symmetry (PDB ID 7S21) from *Myxococcus xanthus*. (G) Archaeoferritin from *Archaeoglobus fulgidus* DSM 4304 (PDB ID 1SQ3). (H) Comparison of subunit alignment of (A) red, (B) green, (C) blue and (G) cyan (the upper part) and the heme in bacterioferritin dimer subunits (D) (the lower part). The structure information is obtained from RCSB and the schematism is generated and processed by PyMol.
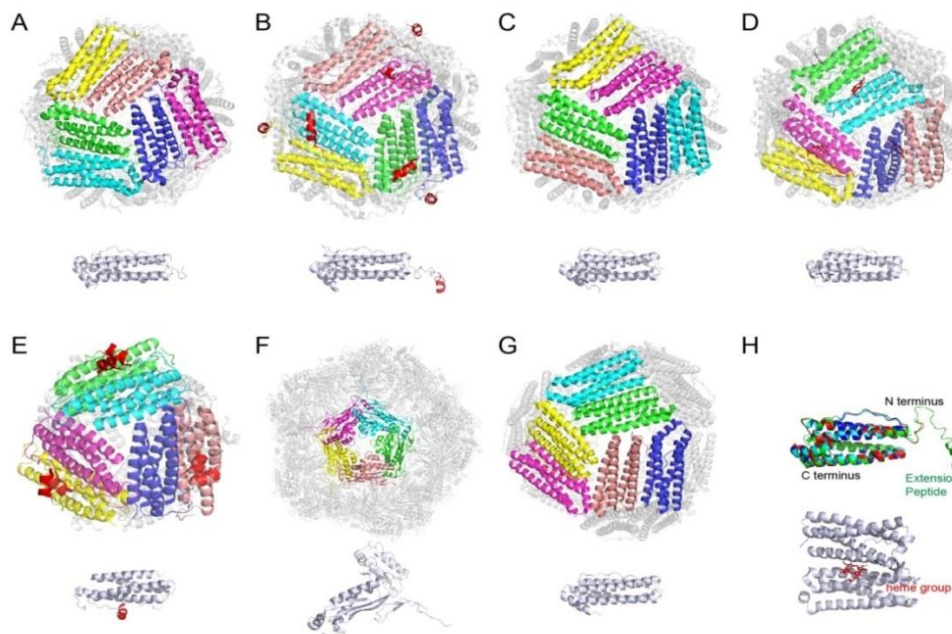

In addition to the natural ferritins, recombinant ferritins have been constructed by self-assembly of different ferritin subunits based on gene and protein recombination engineering and biochemical techniques, which have gotten more use in biotechnology such as delivery system and targeted therapy. For example, the novel chimeric ferritin achieves not only Transferrin Receptor-1 (TfR-1) targeting, but also depolymerization/recombination under mild conditions through recombining human Heavy chain Ferritin (HFn) and archaeal ferritin. It is beneficial to the preparation of intelligent protein and multifunctional, universal and simple protein delivery platforms [51,52].

Location of cargoes in ferritin

Ferritin is an ideal protein carrier for delivering different cargoes, such as contrast agents, chemotherapeutic drugs, nucleic acid drugs and proteins. The nano-spherical cavity structure of ferritin with an inner diameter of 8 nm and an outer diameter of 12 nm can accommodate many small molecules through the channels in ferritin, especially hydrophilic molecules. For macromolecules or hydrophobic small molecules, the encapsulation efficiency is very low through the reversible self-assembly properties of ferritin. However, the encapsulation rate could be improved through chemical or genetic modification of the inner or outer surfaces of ferritin. According to the position of cargo molecules in ferritin, we can divide them into cargo-embedded ferritins, cargo-affixed ferritins and double-interface-modified ferritins (Figures 4A-4C).

Figure 4. The relative position of ferritin and cargo molecules. (A) The cargoes are embedded inside ferritin (cargo-embedded ferritin). (B) The cargoes are loaded on the outer surface of ferritin (cargo-affixed ferritin) (C) The cargoes are presented on the inner and outer surfaces of ferritin (double-surface-modified ferritin). The structure information of protein shell is taken from RCSB (PDB code 6JPS) and processed by PyMOL.
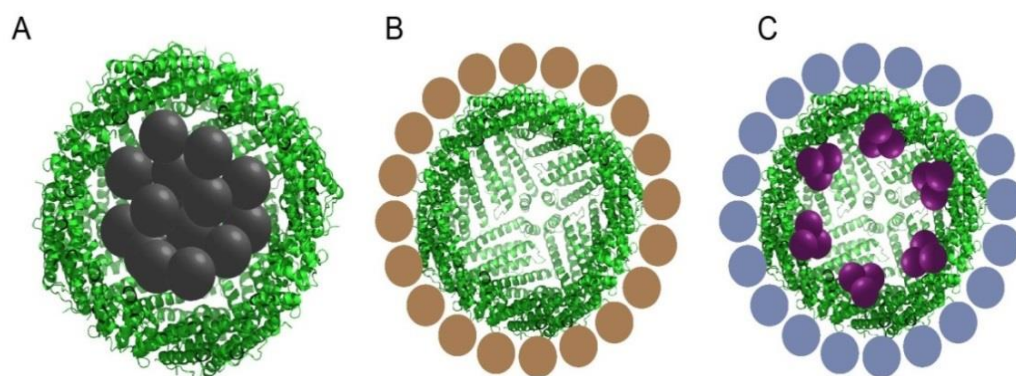
Cargo-embedded ferritin

Channels on the surface of ferritin can be used as transportation routes for tiny cargo molecules. Qualified cargoes with molecular size smaller than pore diameter or high pore affinity can be trapped into ferritin through passive diffusion to form protein-cargo complexes, such as Doxorubicin (Dox), curcumin, and rutin [53,54]. Small molecules can also be encapsulated in ferritin *via* its reversible self-assembly. For example, Dox can be encapsulated in HFn under weakly alkaline/neutral conditions. Compared with using Dox alone, a single dose of Dox-loaded HFn effectively suppressed the growth of tumor without killing normal cells [55]. After encapsulating Dox into ferritin under acidic conditions, the nuclear delivery and the efficacy of chemotherapeutic drug was obviously improved [56]. Ferritin-drug complexes could also be easily prepared by one-step method, due to the passive diffusion of Dox and other small molecule drugs into the cavity through the surface pores of ferritin (Figure 5A (i-vi)) [57].

Ferritin can also deliver proteins/enzymes and agonists [58-61]. The size of the protein or enzyme is larger than the pore diameter of the classical ferritin. They are difficult to be passively transported into the ferritin through the pore channels. However, archaeon *Archaeoglobus fulgidus* Ferritin (AfFtn) has a different architecture with four large triangular pores. Combined with internal negative charges, AfFtn allows substances with larger molecular weight to enter the luminal cavity for loading supercharged protein or protein-enzyme complex, like green fluorescent protein (GFP(+36)) and zinc metalloenzyme Human Carbonic Anhydrase II (hCAII) (Figures 5B and 5C). In addition to loading proteins in ferritin, proteins/enzymes can be co-expressed in ferritin through gene recombination and protein engineering methods [62]. CpG OligoDeoxyNucleotides (CpG ODN), a Toll-like receptor 9 agonist, is not only easily cleared by nuclease during systemic administration, but also tends to induce inflammatory reaction. When HFn is modified with M2 Macrophage targeting Peptide (M2pep) and a piece of Cation Peptide (CP) at the N-terminus and C-terminus, respectively, CpG could be wrapped in ferritin to form M2pep-HFn-CpG NanoParticles (NPs) through reversible assembly of HFn and electrostatic interaction between CpG and CP (Figure 5D). The M2pep-HFn-CpG NPs could effectively polarize macrophages from M2 type to M1 type *in vitro* and showed a strong anti-tumor effect in 4T1 tumor-bearing mice *in vivo*.

Figure 5. The cargos embed inside ferritins. (A) Computational analysis of Dox entering the interior of ferritin through its 4-fold channels over time. (B) Schematic illustration of AfFtn wrapping positively charged GFP variant (green). (C) Diagram of AfFtn encapsulate the designed hCAII(+21). (D) Illustration of the M2pep-rHF construction, M2pep peptide and CP peptide are modified at the N-terminus and C-terminus of rHF, respectively [57,59-61].
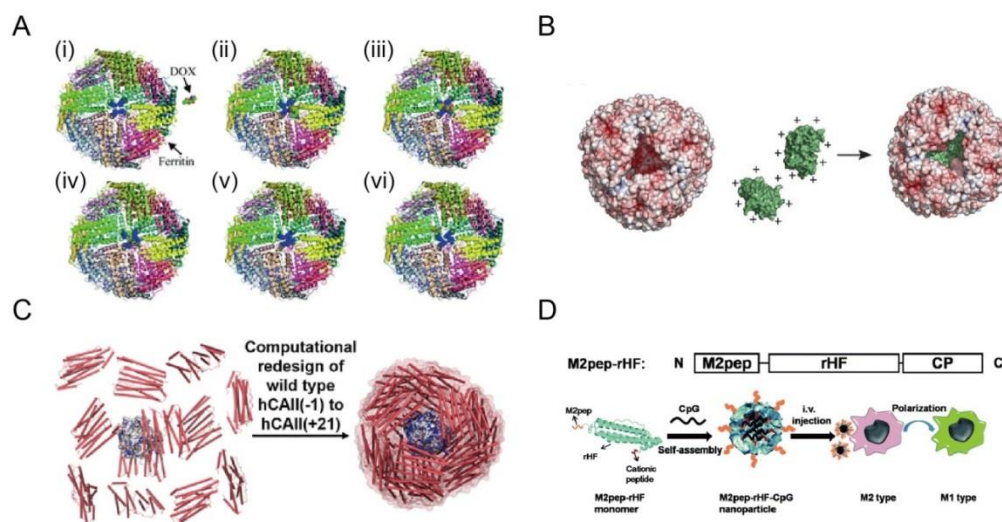
Cargo-affixed ferritin

The presence of abundant amino acid residues on the surface of ferritin is very useful for connecting guest molecules through covalent/non-covalent bonds or gene/protein engineering. The signal-regulating protein α (SIRPα) could be conjugated at the C-terminus of the human ferritin subunit by a flexible chain and presented a natural dimer-like structure on the four-fold channels of ferritin, namely FHSIRPα (Figure 6A) [63-66]. Compared with the Signal-Regulated Protein alpha monomer (mSIRPα), FHSIRPα exhibited superiority in increasing binding affinity for CD47 (integrin-associated protein) to avoid the recognition of macrophages, enhancing phagocytosis of phagocytes, and promoting tumor killing. Another example is the display of antigens on the surface of ferritin. Wang, et al. used the SpyCatcher/SpyTag technique to connect the Receptor Binding Domain (RBD) of SARS-CoV-2 to the N-terminus of *Helicobacter pylori* Ferritin (HpFtn) and formed the RBD trimeric ferritin complex (Figure 6B) [67]. The prepared NPs can inhibit the binding of RBD and hCEA2 *in vitro*. In the case of authentic virus infection, when the complex was combined with Sigma/AddaVax adjuvant, the concentration of neutralizing antibody in serum was 120-fold higher than that using monomeric RBD vaccine.

Figure 6. The cargos affix on the outer surface of ferritins. (A) Illustration of FHSIRPα construction, SIRPα ligand is connected at C-terminus of HFn subunits through a flexible chain, and then self-assembles to FHSIRPα. (B) Schematic representation of RBD-conjugated NP designed through SpyCatch/SpyTag Technique [63,64].
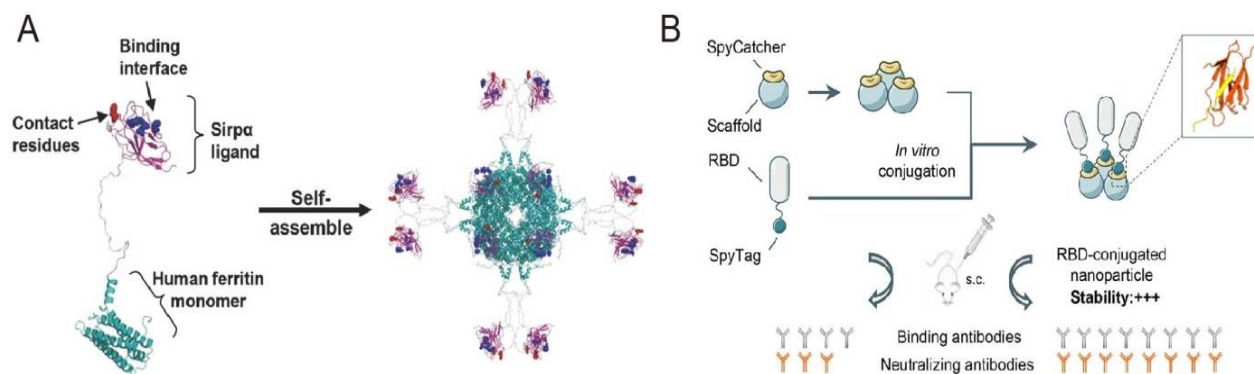
Double-surface-modified ferritin

When loading cargoes on the surface of ferritin, the internal cavity can simultaneously be used to load other cargoes. Thus, the fixation of cargoes on the surface of ferritin is often combined with the loading of the internal cavity. After the surface modification of ferritin, small molecule drugs and biological active compounds can be loaded on the outer surface of ferritin and enter its inner cavity, respectively [65,66]. Wang, et al. replaced the E-helix sequence of HFn with a hydrophobic/hydrophilic peptide motif containing an RGD sequence that targets integrin αvβ3 by gene fusion [67]. The modified ferritin (Am-PNCage) can embed 132 epirubicin molecules in the hydrophilic cavity and affix 50 camptothecin molecules on the outer surface through hydrophobic interaction, which can realize the cascade release of hydrophilic/hydrophobic drugs and kill drug-resistant tumor cells (Figure 7A). investigated the binding kinetics of the peptide to the receptor by displaying the PD-L1 binding peptide sequence at different position of helix V-deleted ferritin [68]. The results showed that PD-L1 binding peptides ligated onto the N-terminus of ferritin (PpNF) exhibited high binding affinity and specificity (Figure 7B). Combined with Dox inside ferritin nanocage, the antitumor activity of doxorubicin-loaded PpNF was effectively enhanced.

The outer surface of ferritins without any modification can also serve as an attachment point for binding guest molecules. Salvianolic acid B could be directly attached to the outer interface of Soybean Ferritin (SFt) through weak bonds, leading to the stability of unstable Epigallo Catechin Gallate (EGCG) embedded in the expanded the four-fold channel was increased (Figure 7C) [69]. Similarly, two different bioactive compounds (i.e., hesperetin and quercetin) were conjugated and encapsulated to the outer and inner surface of phytoferritin by covalent and non-covalent binding, respectively (Figure 7D) [70]. After covalent binding of hesperetin, the modified ferritin retaining the cage-like structure exhibited digestive stability and reversible self-assembly property regulated by pH shifts.

Applications of ferritins

As a natural macromolecule, ferritin possesses unique physical and chemical properties, such as good biocompatibility and high stability to temperature and denaturants, which makes it an ideal platform in many fields. Here, we focus on the application of ferritin in the biosynthesis, sensing, drug delivery, and disease treatment in the recent years.

Template for biosynthesis: Ferritin nanocage is an excellent template for the biosynthesis of NPs, due to the symmetrically three-dimensional structure, hydrophilic/hydrophobic channels and reversible self-assembly and uniform size [71-73]. Compared with chemical synthesis, the biomimetic synthesized NPs by ferritin exhibits the advantages of more uniform particle size, the simpler and greener synthesis process, and higher yields. Metal ions could enter the internal cavity of ferritin through surface channels, and then are reduced to metal particles by the di-iron oxidase on the subunits. The prepared metal NPs can be used as the active center of the enzyme with various activities. Zhang, et al. synthesized Manganese dioxide (MnO_2) core *in situ* to form a pseudo-enzyme by adding $MnCl_2/FeCl_2$ solution and Triphenylphosphonium (TPP) modified on the outer surface of ferritin (Figure 8A) [74]. This hybrid enzyme was able to enhance the activities of Superoxide Dismutase (SOD) and Catalase (CAT), reduce the activity of Peroxidase (POD) in cells, and significantly improve the oxidative damage of mitochondria and the functional recovery of heart injury (Figure 8B).

Figure 7. The cargos present on the inner and outer surfaces of ferritins. (A) Schematic illustration of the EPI@Am-PNCage/CPT NPs preparation. (B) Illustration and 3D model of the PD-L1pep1-ferritin nanocage with different displaying methods. (C) Schematic illustration of the ferritin-salvianolic acid B-epigallocatechin gallate three-layer NPs preparation. (D) Schematic illustration of the ferritin binding two bioactive compounds [67-70].
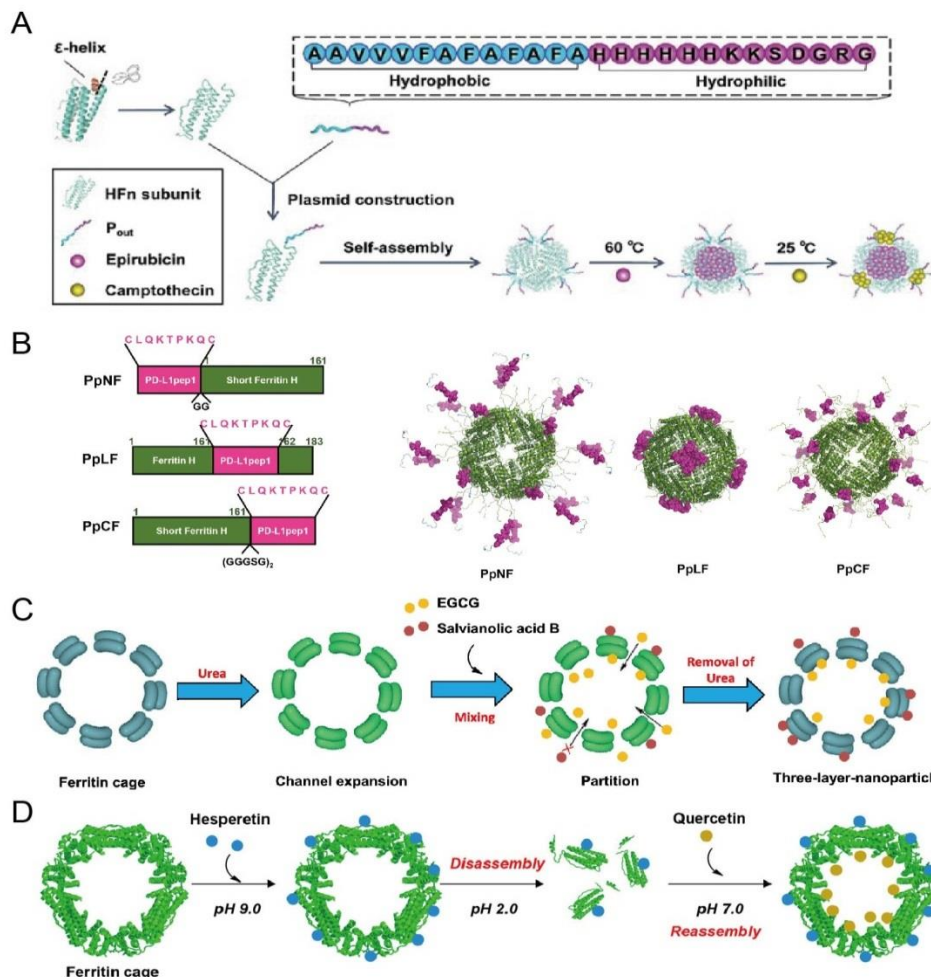
Figure 8. Biosynthesis inside ferritins. (A) Schematic illustration of Mito-Fenozyme preparation and (B) its high POD- and CAT-like enzyme activity to convert superoxide anion to H_2O and oxygen, and lower POD-like enzyme activity to generate hydroxyl radicals [74].
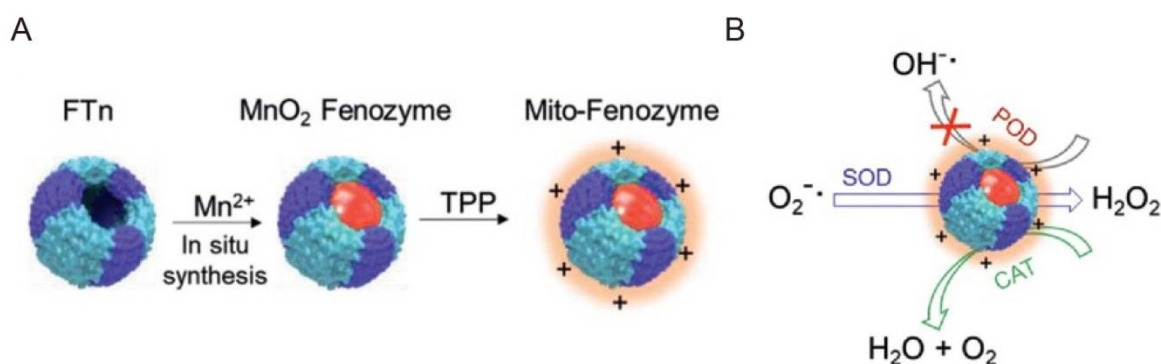
Improvement of analytical performance: Excellent sensitivity, reproducibility and specificity are significantly important to an analytical method. As the gold standard for accurate diagnosis of disease-related markers, Enzyme-Linked Immunosorbent Assay (ELISA) often suffers several disadvantages, such as time consumption, poor linearity and reproducibility, due to the sophisticated operation process and the vulnerability of proteins to the environment. Therefore, many efforts have been dedicated to improve ELISA or develop ELISA-like methods. A kind of ELISA with ferritin substitute antigen-antibody system was designed for clinical diagnosis of autoimmune disease (Figure 9A)

[75]. Compared with commercial ELISA, the sensitivity of ferritin-based capture and detection system was improved by 100 times. In early diagnosis, ELISA is often limited by insufficient sensitivity. Cardiac troponin I (cTn I) is a marker of Acute Myocardial Infarction (AMI) [76]. In order to reduce the death caused by heart disease, the detection sensitivity of cTn I in serum is one of the key parameters for early diagnosis. Men, et al. grafted 24 biotins on the outer surface of ferritin by gene fusion, and then multiple streptavidin modified horseradish peroxidase were combined with biotinylated ferritin to form Enzyme Nano Composite (ENCs), resulting in signal enhancement (Figure 9B (i,ii)) [77]. Compared with the ELISA kit, the sensitivity to cTn I is increased by 10,000 times.

As the technology of combining electrochemical assay and immunoassay, electrochemical immunoassay (ECIA) and Electro Chemi Luminescence Immunoassay (ECLIA) have the characteristics of fast analysis speed, simple steps, high sensitivity and wide application range. Akanda and his co-worker introduced the ferritin-hydrogen peroxide redox system into ECIA and selected ruthenium hexamine ($Ru(HN_3)_6^{3+}$) electrochemical redox pair as the medium (Figure 9C (i,ii)) [78]. In the analysis of antigen from *Escherichia coli* (*E. coli*), the established ECIA system exhibited a good linear range from 10.0 pg/mL to 0.1 µg/mL, and the limit of detection was 10.0 fg/mL. Embedding the luminescent complex of ECLIA in ferritin can effectively improve its water solubility, and even realize the use of non-water-soluble ECL reactive substances in biosensors and immunoassays. For instance, after the insoluble iridium complex was encapsulated in horse spleen ferritin, the aggregation caused by intermolecular interaction was reduced due to the enhanced water solubility (Figure 9D (i,ii)) [79].

Bioimaging: Bioimaging techniques commonly used in clinical practice, such as Fluorescence Imaging (FLI), Bioluminescence Imaging (BLI), Computed Tomography (CT), Positron Emission Tomography (PET) and Magnetic Resonance Imaging (MRI), can provide structural and functional information for the diagnosis and treatment of diseases. Ferritin has become an ideal imaging platform because of its biocompatibility and ability to be modified through protein engineering or chemical modification [80-83].

 A fluorescent probe of luciferin-labeled HFn (Luc-linker@HFn) was designed by connecting luciferin molecules to the outer surface of HFn through disulfide bond in synthetic flexible chains (Figure 10A). In tumor high glutathione microenvironment, free fluorescein was released with the break of disulfide bonds and cyclization of flexible chains. Meanwhile, Luc-linker@HFn could co-deliver drugs to achieve visualized therapy of tumors [84]. With the same strategy, technetium 99m (^{99m}Tc) chemically modified on the outer surface of HFn was used to quantitatively image the vulnerable plaques of atherosclerosis with high specificity, due to the active targeting of ferritin to TfR-1 expressed on the cell membrane of macrophages [85]. Ferritin-based nanoprobe could also be used for selective detection of cells. Liu, et al. fixed hemin, the active site of peroxidase, inside HFn to form hemin@HFn, based on disassembly/reassembly of ferritin at different pH (Figure 10B). After embedding hemin, the peroxidase activity and tolerance to high temperature or denaturants of hemin@HFn were both enhanced [86]. Moreover, hemin@HFn can target HeLa cells and oxidize 3,3',5,5'-Tetramethylbenzidine (TMB) in the cell for colorimetric detection. The detection limit of this colorimetric assay was as low as 125 cells, and good linearity was shown below 2000 cells with the correlation coefficient R^2=0.997.

Figure 9. Analytical applications of ferritins. (A) The representative diagram of ferritin-based capture-detection ELISA-like assay. (B) Construction of ENCs. (i) The representative diagram of an ENC-based high-sensitivity immunoassay. (ii) Preparation of ENCs with biotinylated ferritin and SA-HRP. (C) (i) The principle and (ii) detection process of ferritin-based OSR/ISR redox cycling system. (D) (i) Design and detection procedure of ferritin-based immunosensor without $Ti_3C_2T_X/TiO_2$ and (ii) with $Ti_3C_2T_X/TiO_2$ [75,77-79].
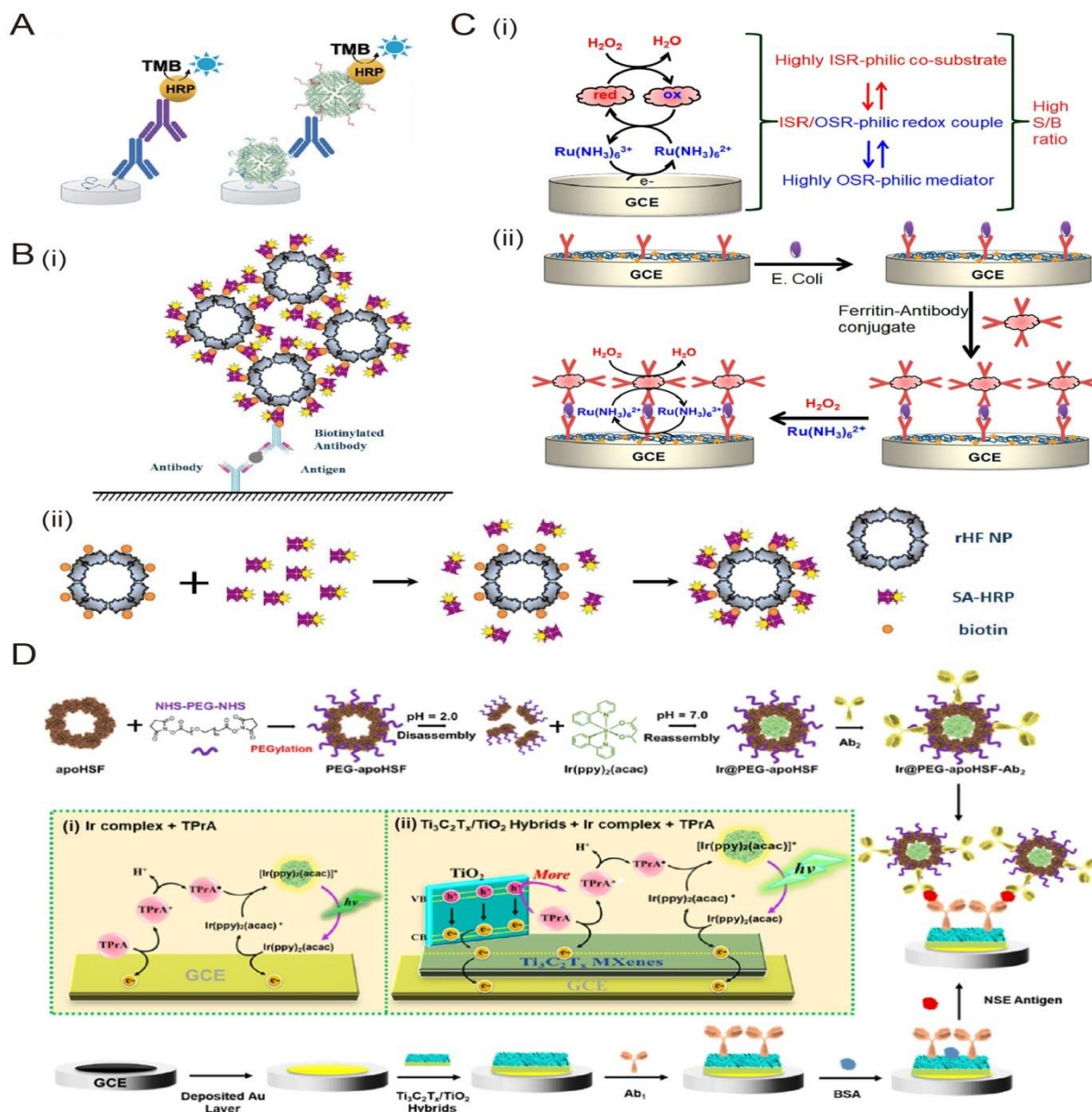
Multimodality imaging is one of the methods to improve the accuracy and sensitivity of imaging. Ferritin can embed Contrast Agents (CAs), radionuclides or photosensitizers in the cavity through self-assembly process and connect fluorescent dye molecules to subunits by chemical or gene modification, thus establishing a multimodality imaging method. Based on this strategy, a two-mode imaging method with RGD targeting was constructed by combining Near-Infrared Fluorescence (NIRF) imaging and Positron Emission Tomography (PET) imaging [87,88]. Cy5.5 and ^{64}Cu were used as dye molecules and nuclide, respectively (Figure 10C). In order to reduce the chemical cross-reaction during connecting RGD and Cy5.5, ferritins modified with RGD or Cy5.5 were prepared separately, and then multifunctional chimeric ferritin was prepared through the hybridization of these two types of modified ferritins and encapsulating ^{64}Cu. Similarly, NPs named IRDye800-M-HFn are designed by connecting photosensitizer IRdye800 to ferritin surface and synthesizing iron oxide core. IRDye800-M-HFn can realize the three-mode imaging of photo acoustic (PA), NIRF and nuclear Magnetic Resonance (MR), so as to realize the early diagnosis and treatment of tumors [89].

Figure 10. Ferritin-based bioimaging. (A) Structure of luciferin-ferritin complex. (B) Preparation process of hemin@HFn NPs by reversible self-assembly of HFn. (C) Schematic diagram of ferritin-based multimodality imaging probe [84,86,88].
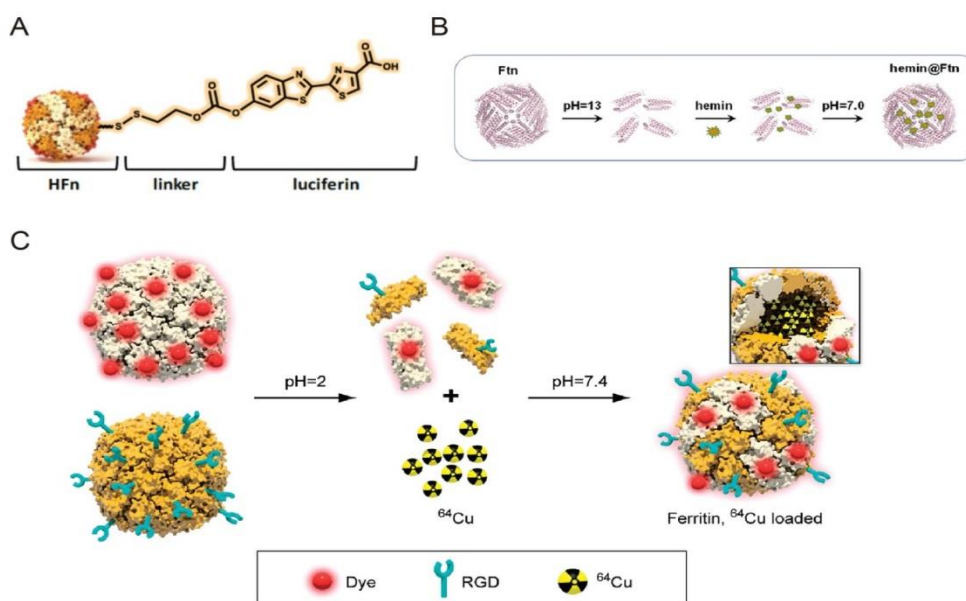

Therapy: At present, targeted/individualized therapy and some novel therapeutic treatments have attracted more and more attention, like phototherapy, thermotherapy, immunotherapy and gene therapy, etc. For ferritin, in addition to actively targeting TfR-1 for tumor diagnosis and treatment, its cage-like structure with multiple interfaces and reversible self-assembly allow for the encapsulation and delivery of biologically active molecules [90]. For example, the targeting motifs can be modified on the surface of ferritin to enhance its targeting ability or endow it with a new targeting ability. Thus, ferritin is a good choice as a nano-carrier for drug delivery.

Chemotherapy: Conventional chemotherapy results in non-targeting, high toxin-side effects and short blood half-life. Therefore, the development of a drug vehicle to enhance drug targeting, reduce drug poison side effect, and prolong drug action time is one of the solutions. In order to increase the targeting ability of Pyrococcus Furiosus Ferritin (PfFtn) to Hepatocellular Carcinoma (HCC), Jiang, et al. connect SP94 to the N-terminus of PfFtn by genetic engineering, which could specifically bind to the glucose-regulated protein GRP78 on the membrane of HCC [91]. The GRP78-targeted ferritin nanocage (HccFtn) can load ultra-high dose Dox through disassembly/reassembly, which can reduce the damage of free Dox to healthy tissue and effectively kill subcutaneous and lung metastatic HCC (Figure 11A (i,ii)). Similarly, for enhancing the cellular targeting and penetration of HFn, a flexible chain was used to connect the C-terminus of HFn and a neuropilin-1 (NRP-1) binding peptide (RGERPPR) which can target NRP-1 receptor on the surface of neovascular endothelial cells and cancer cells [92]. With loading Paclitaxel (PTX), the formed NPs was proved to have excellent cell penetration and tumor suppression in the 3D cell sphere of A549 (human lung carcinoma cells) (Figure 11B (i-iii)). The group also prepared functionalized ferritin nanoparticles that can inhibit the Mitogen-Activated Protein Kinase/Extracellular Signal-Regulated kinase (MAPA/ERK) pathway by the same way [93]. They connect ERK peptide inhibitor, a 13 amino acids peptide (MPKKKPTPIQLNP) at the N-terminus of MAPK/ERK kinase (MEK), to the C-terminus of HFn to form HERK particles. Meanwhile, PTX is loaded inside ferritin to form HERK-PTX particles based on the pore expansion of HFn at low concentration urea. Under the synergistic effect of the inhibitor and PTX, the therapeutic effect of HERK-PTX was improved with enhanced cellular

uptake (Figure 11C (i,ii)). In addition to being a carrier to deliver cargo molecules, ferritin can be used as a targeting motif of other carriers to enhance the targeting ability, due to its ability to naturally target TfR-1. For example, Horse Spleen Ferritin (hsFtn) is covalently modified the outside of inhibitor doped poly (lactic-co-glycolic acid) polymer nanoparticles by NHS groups to achieve TfR-1 mediated endocytosis [94]. Furthermore, ferritin can be used as both a capping agent and a targeting agent. After combining HFn on the surface of Mesoporous Silica Nanoparticles (MSN) by disulfide bond, Dox is efficiently blocked in the pores of MSN to prevent from diffusing out, and delivered to malignant cells by binding HFn to the TfR1 that has been overexpressed in various tumors [95].

Figure 11. Construction of ferritin-chemotherapeutic drug complex. (A) (i) Schematic illustration of HccFn-Dox NPs preparation, and (ii) The survival curve graph of liver cancer mouse model after HccFn-Dox formulation therapy. (B) (i) Illustration of HFtn-MMP2-RGE or HFtn-mMMP2-RGE subunit and 3D model and (ii) Design, and (iii) The volume change of A549 tumor spheroid after different formulations treatment. (C) (i) Schematic diagram of the HFn subunit with the ERK peptide linked to the C-terminus. (ii) The volume change of tumor spheroid after different preparations therapy. **NOTE:** A (ii) (⟶) HooFn; (⟶) Doxil; (⟶) HccFn-Dox; (⟶) Dox; (⟶) PBS, B(iii) (⟶) DMEM; (⟶) PTX; (⟶) HFtn-PTX; (⟶) HFtn-mMMP2-RGE-PTX, C (iii) (⟶) Control; (⟶) PTX; (⟶) HFtn-PTX; (⟶) HERK-PTX [91-93].
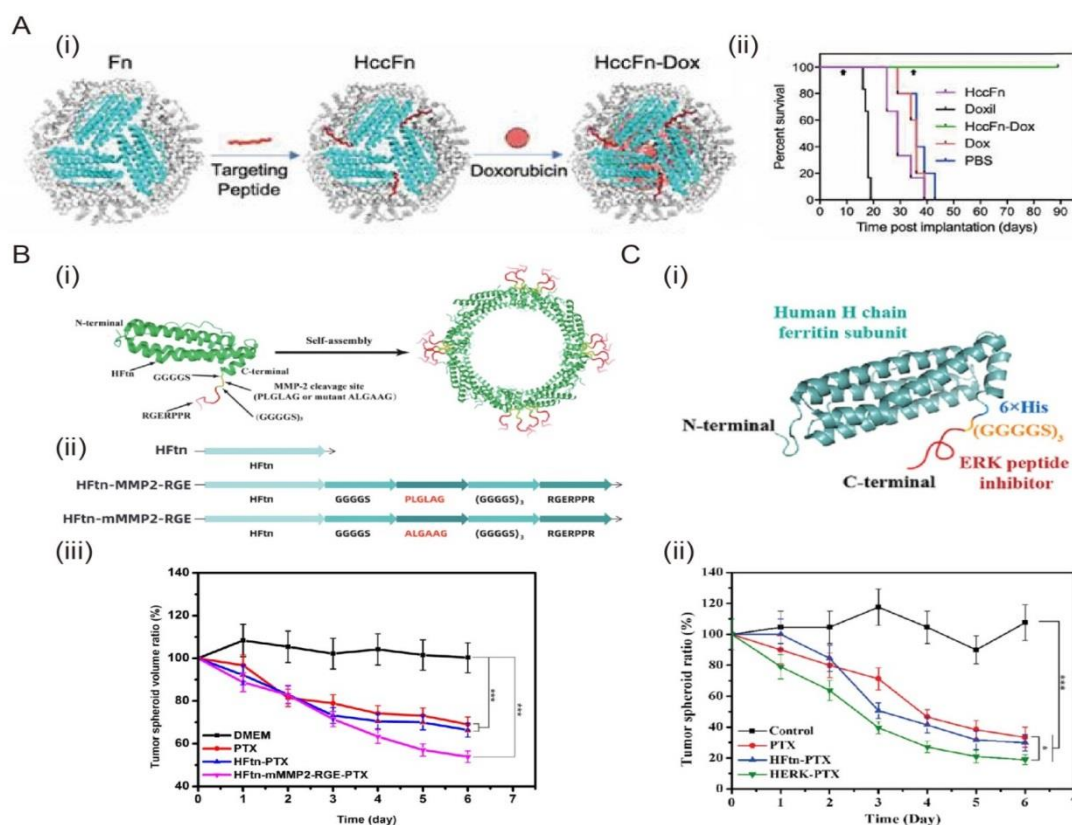
Gene therapy: Gene therapy can alleviate or treat many diseases that cannot be treated by traditional methods, such as gene mutations, chromosome mutations or protein abnormalities. Nucleic Acid Drugs (NADs) that silence or repair disease-related genes are delivered to the cytoplasm or nucleus to achieve gene therapy of diseases. NADs are generally oligonucleotides or oligodeoxynucleotides. The exposed NADs are easy to be degraded by nucleases, so the effect of using NADs alone to treat diseases is very poor. Generally, NADs need to be modified or added carriers to increase the stability or targeting ability. The commonly used nucleic acid carriers are divided into viral vectors and non-viral vectors; the former has safety problems, while ferritin, as an endogenous protein in the

human body, has exceptional biosafety and biocompatibility. The internal cavity can also hold nucleic acid drugs. Thus, ferritin is an ideal NAD delivery vehicle.

Compared with other nucleic acid drugs, siRNA can target gene without any limit, and the gene silencing time is longer. However, naked siRNA is easily degraded by endogenous nuclease, and the cell membrane penetration is poor due to its rich negative charge and large size. Therefore, it is necessary to find a suitable vehicle to improve enzyme stability and cell uptake of siRNA. In previous reports, HFn expressing Cell Targeted Peptide (CTP), Cell Penetrating Peptide (CPP), Cationic Peptide (CAP) and Enzymatically Cleaved Peptide (ECP) by gene modification have been used for carrying siRNA (Figure 12A). The tunable of CTP and siRNA makes siRNA-ferritin polymer promising to become a general platform for cancer gene therapy. siRNA could be contacted with CAP on the HFn by electrostatic interaction to form siRNA-ferritin complex, after siRNA is polymerized by sulfhydryl groups at the 5' end of each siRNA. The good ability of cell targeting/penetration and gene silencing of siRNA-ferritin are verified in MDA-MB-468 (human breast cancer cells) and B16F10 (mouse melanoma cells) [96].

The internal cavity of ferritin is negatively charged and has electrostatic repulsion with negatively charged siRNA, but the self-assembly properties of ferritin dependent pH can be used to compress siRNA (Figure 12B) [97]. In addition, it has been reported that the negative charge in ferritin can be ameliorated to deliver siRNA. For example, based on the reaction of sulfhydryl residues in ferritin with maleimide and pentafluorobenzenesulfonamide, Pediconi, et al. connect rigid rod-like amine compounds, piperazine-piperidine compounds, to the interior of "Humanized" chimeric Archaeal Ferritin (HumAfFtn) for preparation of the amine-modified ferritin (Figure 12C) [98]. This cationic decorated ferritin can be reversibly self-assembled in salt solution (such as magnesium chloride), thus loading siRNA that can silence the expression of Glyceraldehyde-3-Phosphate Dehydrogenase (GAPDH) gene. With TfR-1 receptor-mediated uptake, siRNA encapsulated in ferritin can reduce the key enzyme expression of glycolysis, GAPDH, in HeLa, HepG2, and MCF-7 cells. A similar strategy is used to deliver pre-miRNA. Different generations of Polyamide-Amine Dendrimers (PAMAM) were screened to induce HumAfFtn polymerization and prepared PAMAM-HumAfFtn complex (Figure 12D) [99]. Based on the electrostatic interaction, pre-miRNA enters the interior of PAMAM-HumAfFtn through four triangular pores on the surface of ferritin to form protein-amine-nucleic acid ternary complex. The complex can be absorbed by Acute Myeloid Leukemia (AML) cells, resulting in changes in cell phenotype and morphology. Changing the internal charge of ferritin can make ferritin an ideal vehicle for NADs delivery, but the drug loading rate and behavior *in vivo* need to be further investigated. The acidic environment and many proteases in endosomes/lysosomes will cause irreversible damage to the siRNA and ferritin. In order to perform the function of siRNA-ferritin complex in the cytoplasm, some researchers use the modified ferritin or add some agents to exert lysosome escape of the complex. For instance, when calcium ion (Ca^{2+}) and phosphate salt are added during the process of loading siRNA by pH-dependent HFn self-assembly. Not only Ca^{2+} can neutralize part of the negative charges of siRNA, but also the hydrolysis of calcium phosphide mineralized in HFn can play the role of proton sponge, leading to the release of siRNA from lysosome to cytoplasm. After adding Ca^{2+}, the intracellular internalization rate of siRNA increased by 1.65 times, which could enhance the anti-tumor effect in 4T1 tumor mouse model [100]. In addition, this team modified four lysines to the N-terminus of HFn through genetic modification, namely poly (L-lysine) modified H-chain apoferritin (TL-HFn) (Figure 12E) [101]. TL-HFn can achieve lysosome escape and complete nuclear delivery and nuclear accumulation of drugs, while delivering NADs, chemotherapeutic drugs, or ribonucleoproteins (RNPs) complex [102,103].

Figure 12. Ferritin-based gene vectors. (A) Construction of peptide-modified HFn NPs through gene fused. (B) Illustration of unmodified ferritin-coated siRNA encapsulation procedure. (C) 3D model of siRNA-PAs-HumAfFt. The

ferritin modified with different amino molecules, such as PA2 and PA3 modified *via* the reaction between sulfhydryl and maleimide or pentafluorobenzenesulfonamide. (D) Schematic illustration of ferritin-dendrimer NPs preparation. (E) Schematic illustration of tetralysine-modified ferritin for siRNA delivery and treatment [96-99,101].
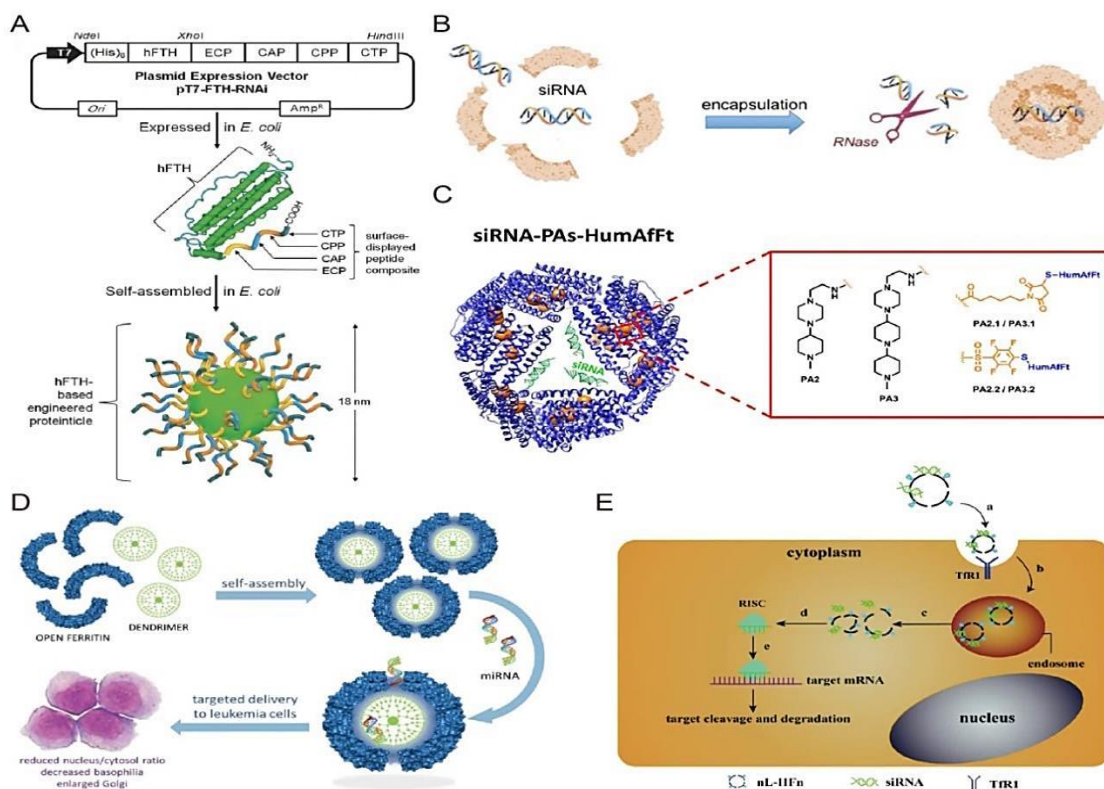

Vaccine and immunotherapy: Traditional vaccine production is a time-consuming and sophisticated process [104]. How to easily and stably prepare on a large scale is the key point to solve the problem of vaccine generation. In biotechnology and protein surface engineering, SpyCatcher-SpyTag technology and Intein trans-splicing technique are often used to covalently bind Proteins of Interest (POI), which have sparked widespread concern in vaccine development. Ferritin has ample amino acid residues on its surfaces and is an endogenous macromolecular protein, so it can be modified with various antigens/haptens to enhance their antigenicity and immunogenicity. And the antigens insertion in C-terminal region of ferritin has fewer hydrophobic surfaces and is more tolerant to the environment (e.g., stability, pH, chemical denaturants, etc.) than the insertion in N-terminal region [105]. More importantly, ferritin will not cause an immune response itself. Thus, ferritin-based NPs are expected to be used in vaccine manufacturing and immunotherapy. At present, the ferritin-based H2 influenza nanoparticle vaccine (NCT03186781) has entered phase I clinical trials, demonstrating the feasibility of ferritin for vaccine design [106]. Han, et al. introduced antigenic peptides OT-1 (SIINFEKL) or OT-2 (ISQAVHAAHAEINEAGR), which can bind to OVA-like epitope receptors on CD8+ and CD4+ T cells, into C-terminus or middle loops of PfFtn by gene fusion [107]. The prepared NPs (OT-FPCN) can not only induce the proliferation of CD8+ and CD4+ T cells *in vivo* and *in vitro*, but also promote the differentiation of CD8+ T cells into effector T cells and CD4+ T cells into Th1/Th2 T cells. Severe Acute Respiratory Syndrome-2 (SARA-2) caused by the Coronavirus has caused great panic around the world. Up to now, the global epidemic is still very serious. Structured-based ferritin vaccines against SARA-CoV-2 have attracted the attentions of scientists, mainly for the SARA-CoV-2 Spike Protein (Sp), whose RBD can bind to Human Angiotensin Converting Enzyme 2 (hACE2), thereby mediating viral invasion [108]. In non-human primates (rhesus macaques), the

combination of RBD-ferritin nanoparticle vaccine (RFN) or Sp-Ferritin Nanoparticle vaccine (SpFN) with the immune Adjuvant army liposomal Formulation QS-21 (AFLQ) can produce potent Th1 CD4+ T cell responses and cell-mediated immune response [109,110]. Moreover, it is highly protective against upper and lower respiratory airways and lung parenchyma stimulated under high doses of SARA-CoV-2 by reducing viral replication and has a strong specific immune response to heterologous SARA-CoV-1. The above results indicate that the ferritin nanoparticle vaccine designed for the SARA-CoV-2 spike protein or RBD region has a strong immunotherapy effect on SARA caused by β-coronavirus and is an excellent candidate vaccine. Conventional SpyCatcher molecule has a large molecular weight and strong immunogenicity. By optimizing the structure of SpyCatcher (e.g., deleting N-terminal 24-47 amino acids and /or C-terminal 121-138 amino acids, named SpyCatcherΔN and SpyCatcherΔNC), the obtained SpyCatcher/SpyTag system is very practical for the design and preparation of ferritin nanoparticle vaccines. Wang, et al. separately linked SpyCatcherΔN and G_4S linkers to the N-terminus of PfFtn, SpyTag to the C-terminus of HPV6 oncogene E7 peptide or E7 neoantigen, and SpyTag to the C-terminus of MC38 mutant neoantigen by protein fusion technology [111]. Through the interaction of SpyCatcher and SpyTag, the ferritin-E7/E7 (43-62) nanoparticle vaccine is formed. In C57BL/6 mice, TC-1 and MC38 tumor models, ferritin-E7/E7 (43-62) have a strong effect on inducing Cytotoxic T Lymphocyte (CTL) and tumor suppression. In addition, ferritin-E7/E7 (43-62) can also have a synergistic effect with checkpoint inhibitors (e.g., PD-1, PDL-1) to produce an anti-tumor effect, resulting in a precise attack on tumor. Similarly, Ma, et al. linked RBD and/or Heptad Repeat (HR) subunits to the N-terminus of HpFtn to form RBD-ferritin or RBD/HR-ferritin vaccines [112]. For non-human primates, both vaccines could produce more neutralizing antibodies and stronger cellular immunity than the monomer vaccine, which can last for at least three months. For hCEA2 transgenic mice, the two vaccines can reduce the amount of lung virus under SARA-CoV-2 challenge, indicating that the vaccines have a strong preventive effect.

Intein trans-splicing technique can connect two exons and accompany their own excision, which is an important way of post-translational modification [113]. Tang, et al. connected the N-terminus of the intein (intN) to the cargo molecule and the C-terminus of the intein (intC) to HFn using the principle of trans-splicing, and modified intN and intC with the B1 domain of streptococcal protein G tag (gb1 tag) to increase its yield and solubility [114]. The nanoparticles prepared in this way can effectively deliver antigens and adjuvants to antigen-presenting cells and then trigger an effective immune response (Figure 13). Compared with chemical and gene modification methods, inteins mediated trans-splicing has good stability and high coupling efficiency without destroying the architecture of ferritin. More importantly, it can deliver antigens and adjuvants together.

Thermotherapy and photodynamic therapy: In recent years, the heat generated by magnetic materials has attracted a considerable attention in the treatment of solid tumors [115]. Ferritin can be used for magnetic hyperthermia. However, its magnetocaloric effect will be reducing if the mineral core (ferrihydrite) of natural ferritin is wrapped by protein. Studies have shown that the properties of ferritin (like magnetite core size and Fe concentration) could affect the magnetothermal conversion efficiency of magnetoferritin [116]. Meanwhile, the magnetocaloric effect of ferritin could be improved by adding some highly magnetic anisotropic elements to the magnetite core. Cobalt-doped human ferritin nanoparticle was synthesized for magnetothermal therapy of B16 melanoma cells (Figure 14A) [117]. After the modification of its outside surface with PEG and α-melanocyte stimulating hormone (α-MSH), the Co-doped HFn-MSH NPs can bind to the melanocortin receptors and significantly reduce the survival rate of tumor cells *in vitro.*

Figure 13. Ferritin-based vaccine and immunotherapy. Schematic illustration of Sp70/CpG-HFT NPs construction through trans-splicing technique [114].
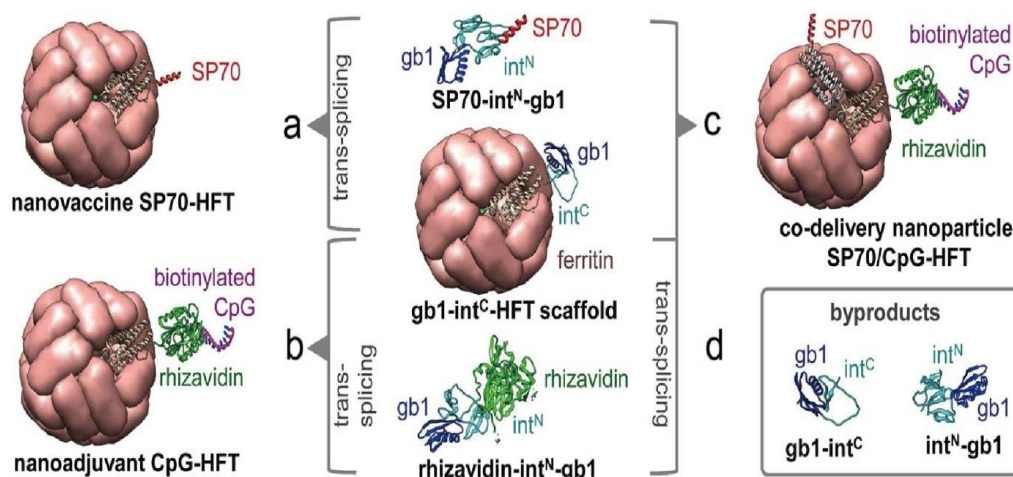
Photodynamic therapy (PDT) is a method of eliminating tumor cells by photoexcitation with reactive oxygen species produced by photosensitizers [118]. For combination of photodynamic therapy and immunotherapy, the Single Chain Variable Fragment (scFv) which can target the Fibroblast-Activation Protein (FAP) overexpressed on Cancer-Associated Fibroblasts (CAFs) is attached to the outer surface of ferritin, and then photosensitizer $ZnF_{16}Pc$ is loaded inside ferritin to form αFAP-Z@FRT (Figure 14B) [119]. It has a strong inhibitory effect on both the initial tumor and the distal tumor in 4T1 mouse model [120]. Liu, et al. used a single-chain variable domain of heavy-chain-only antibodies from camel serum as the targeting motif to construct a nanobody-ferritin platform for targeted drug delivery [121]. After two additional lysine residues were introduced to the N-terminus of HFn to gain active NH_2, the anti-epidermal growth factor receptor (anti-EGFR) nanobody 7D12 modified with Q-tag could be site-specifically linked to the surface of the HFn nanocage by Transglutaminase (mTGase) mediated ligation. With loading 82 photodynamic reagents, manganese phthalocyanine (MnPc), into the cavity of HFn through self-assembly, the resulting system, MnPc@Nb-Ftn can selectively accumulate in and efficiently kill EGFR positive A431 cancer cells upon laser irradiation (Figure 14C). The hypoxia in the tumor area is not conducive to the production of ROSs in PDT. Therefore, the alleviation of hypoxia in the tumor microenvironment is one of the ways to enhance the effect of PDT on tumor treatment. When the nano-formulations prepared by simultaneously wrapping Manganese dioxide (MnO_2) and Chlorin e6 (Ce6) in HFn are accumulated in the tumor site, the catalase activity of MnO_2 can be used to catalyze Hydrogen Peroxide (H_2O_2) to generate Oxygen (O_2) in the slightly acidic TEM (Figure 14D) [122]. With the relief of hypoxia state, the effect of ROS generation from Ce6 is enhanced after laser irradiation.
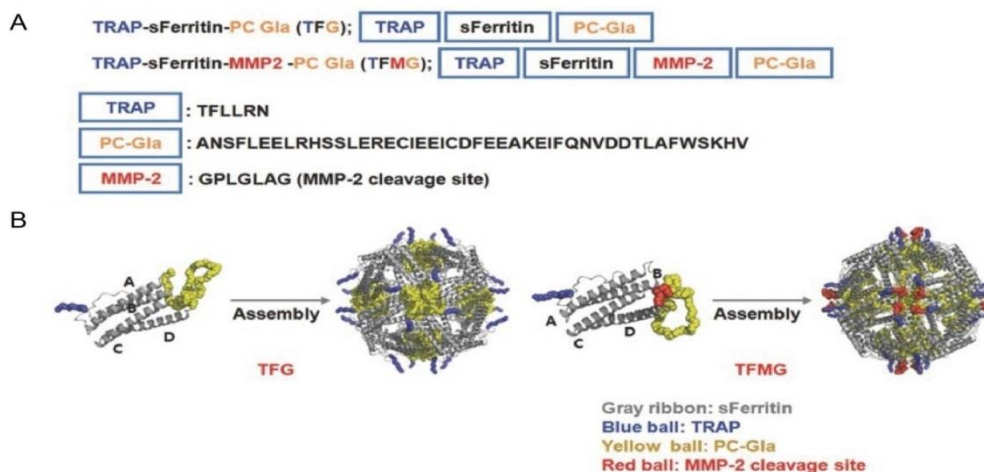
Inflammation therapy

Inflammation is closely related to physiological and pathological processes, and the treatment of inflammation is beneficial to the therapy and recovery of diseases [123]. Ferritin as a carrier of anti-inflammatory drugs can effectively reduce side effects. For instance, Recombinant Activated Protein C (rAPC) is commonly used to cure sepsis. However, rAPC can easily lead to bleeding, which limits its clinical use. Based on the therapeutic mechanism of rAPC. Lee, et al. constructed a Short Ferritin Nanocage (sFn) by deleting the E-helix subunit and loop of light chain for simultaneously loading a γ-carboxyglutamic acid domain of PC/APC (Pc-Gla) and a protease-activated receptor 1 activating peptide (Figures 15A and 15B) [124].

Figure 14. Ferritin in thermotherapy and photodynamic therapy. (A) Preparation process of melanoma targeting and PEGylated ferritin NPs. (B) Mechanistic illustration of FAP-targeted ferritin-mediated photoimmunotherapy. (C)

Preparation process of MnPc@Nb-Ftn NPs and its mechanism of ferritin-based PDT. (D) Mechanistic illustration of Ce6/Ftn@MnO₂ for tumor PDT under FLI and MRI imaging [117,119,121,122].
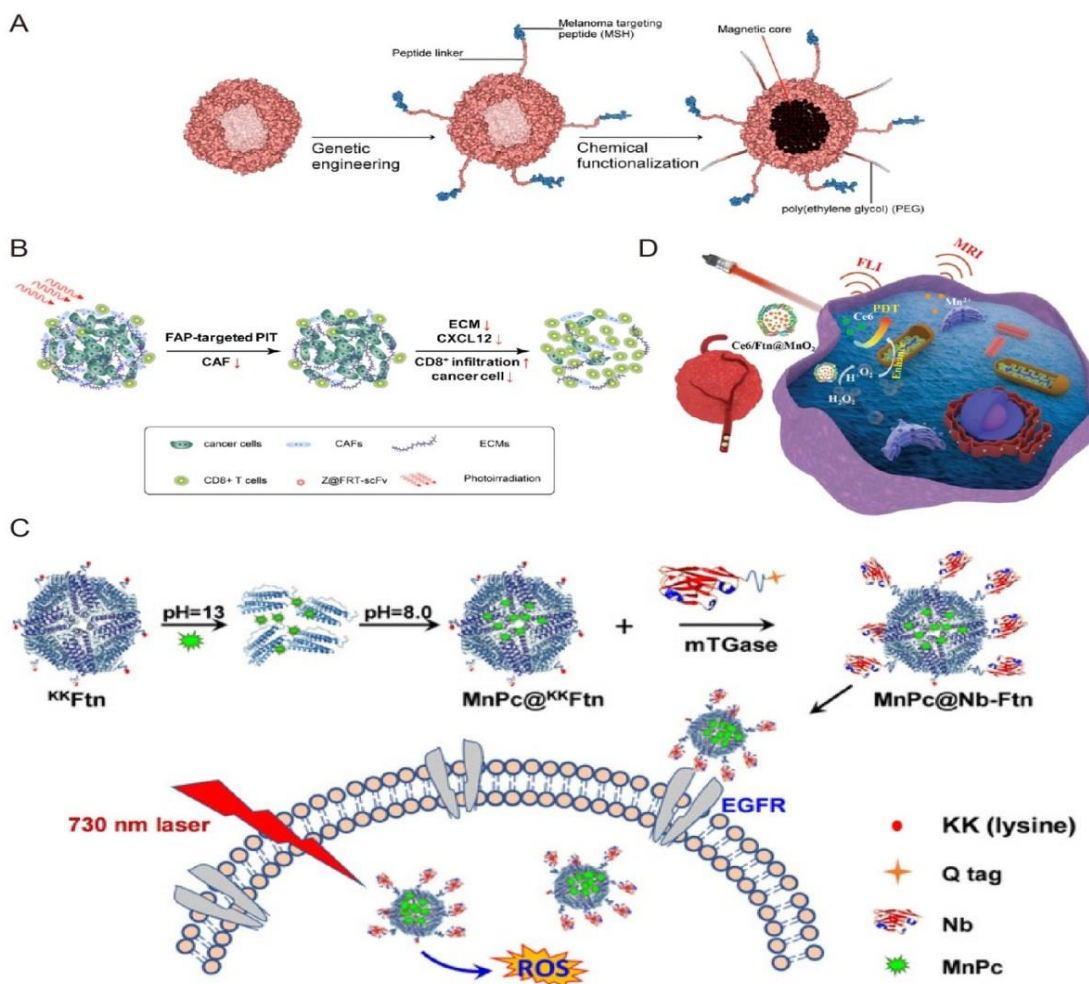
Figure 15. Ferritin-based inflammation therapy. (A) Schematic illustration of TFG and TFMG, and the amino sequence of TRAP, PC-Gla, and MMP-2. (B) 3D model of TFG and TFMG using computer simulation [124].


This kind of double-loaded particles has a good therapeutic effect on vascular inflammation and sepsis without causing bleeding complications. Similarly, a ferritin nanocage was used to carry SET-Domain containing 6 (SETD6)

to maintain its activity *in vivo*. The obtained particles can effectively inhibit Cytokine Release Syndrome (CRS) and NF-κB signaling-mediated inflammatory response. Moreover, if further embedding antiviral drugs, the particles have the potential of being used in the treatment of COVID-19.

DISCUSSION

Ferritin nanocages can also be used as a building block of supramolecular structures to synthesize some novel multi-dimensional nanomaterials from *de novo*, because ferritin can be linearized or self-assembled into larger aggregates through ion-induced aggregation or molecular-induced aggregation [125-127]. For example, multiple ferritins can be linked into an oligomer by the interaction between two-arm Poly Ethylene Glycol (PEG) and pores of ferritin (Figure 16A) [128]. A series of biomimetic nanozymes were prepared by doping metal ions into the cavity of oligomeric ferritin, which has the peroxidase-like function. The experimental results showed that the enzyme activity of platinum-doped oligomeric ferritin was the highest, and its anti-tumor effect *in vivo* was significantly higher than that of nanozyme alone. The nested cage-within-cage (Matryoshka-type) structure prepared with ferritin can be used as reaction chamber or drug carrier. For better self-assembly of ferritin and AaLS-13 (a negatively charged capsid from *Aquifex aeolicus*) to form Matryoshka-type structure, additional arginine and lysine residues were introduced on the outer surface of HFn to increase the positive charge density, leading to higher electrostatic interaction between HFn and AaLS-13 (Figure 16B) [129-131]. Ferritin can also be used to form protein-metal organic frames (protein-MOFs), based on histidine, which is on the outer surface and in the pores of ferritin, coordinating with metal ions. Coupled with ferritin, different metal ions and small organic ligands were investigated to prepare six kinds of protein-MOFs through a modular protein/material design strategy. It is found that the obtained protein-MOFs possessing extremely sparse lattice connectivity might display unusual thermo mechanical properties (Figure 16C (i,ii)).

Figure 16. Ferritin as a building block. (A) Schematic preparation of FTn-Ner using two-armed PEG. (B) Schematic illustration of Matryoshka-type supramolecular structure composed of ferritin and AaLS-13. (C) (i) Schematic illustration of p-bdh-Zn-ferritin. (ii) The organic linking molecules used to connect metal ions and ferritins [128,130,131].
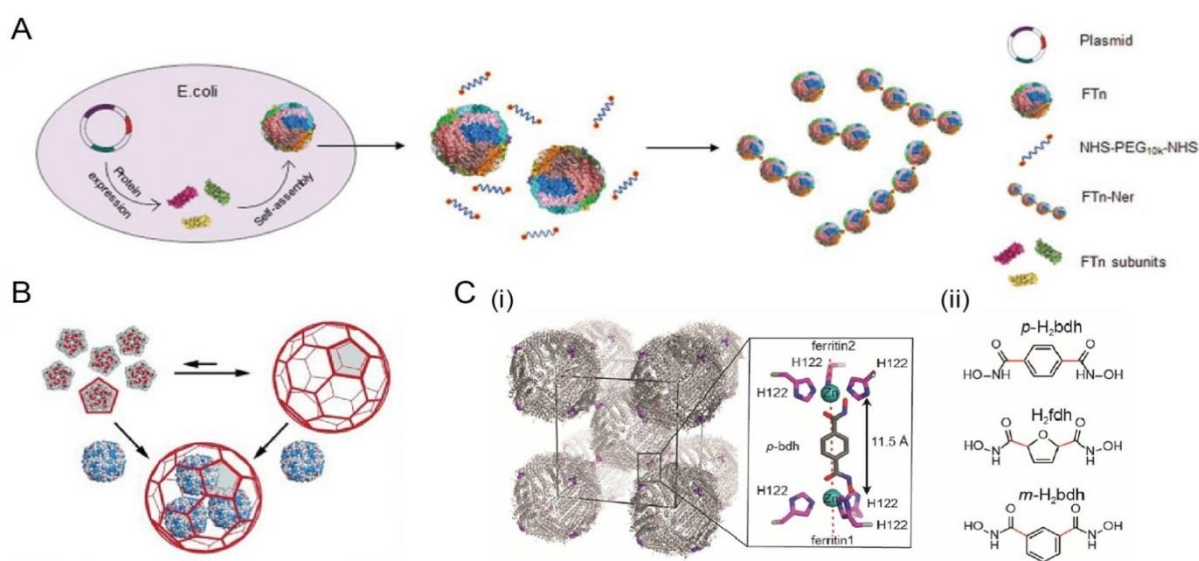
CONCLUSION

As an iron storage protein widely existing in organisms, ferritin has many advantages, such as good biodegradability, low toxicity, good thermal/chemical stability and easy surface modification. Ferritin and its derivatives are promising nano-platforms, especially in the field of drug delivery and bio imaging. This review summarized the recent advances in the synthesis and application of ferritin-based nanomaterials. However, how to avoid the cleavage of ferritin from cargo molecules, how to improve the loading rate or entrapment rate of cargo molecules, and the clinical transformation of ferritin needs to be further studied.

ACKNOWLEDGEMENTS

REFERENCES

1. Theil EC. The ferritin family of iron storage proteins. Adv Enzymol Relat Areas Mol Bio.1963; 63:421-429.

2. Chasteen DN, et al. Mineralization in Ferritin: An efficient means of iron storage. J Struct Biol. 1999;126:182-194.

3. Ayton S, et al. Ferritin levels in the cerebrospinal fluid predict Alzheimer's disease outcomes and are regulated by APOE. Nat Commun. 2015;6:6760.

4. Levi S, et al. Neuroferritinopathy: From ferritin structure modification to pathogenetic mechanism, Neurobiol Dis. 2015;81:134-143.

5. Zhang N, et al. New insights into the role of ferritin in iron homeostasis and neurodegenerative diseases. Mol Neurobiol. 2021;58:2812-2823.

6. Muhoberac BB, et al. Iron, ferritin, hereditary ferritinopathy, and neurodegeneration. Front Neurosci. 2019;13: 1195.

7. Nugzar O, et al. The role of ferritin and adiponectin as predictors of cartilage damage assessed by arthroscopy in patients with symptomatic knee osteoarthritis. Best Pract Res Clin Rheumatol. 2018;32:662-668.

8. Ganz T, et al. Anemia of inflammation. N Engl J Med. 2019;381:1148-1157.

9. Mahroum N, et al. Ferritin from iron through inflammation and autoimmunity to COVID-19. J Autoimmun. 2022; 126:102778.

10. Zhang Y, et al. Ferritin light chain: A candidate autoantigen in immuno-related pancytopenia. Front Immunol. 2022;13:851096.

11. Carmona F, et al. Chemically and biologically harmless versus harmful ferritin/copper-metallothionein couples. Chem Eur J. 2015;21:808-813.

12. Li L, et al. Comparison of two endogenous delivery agents in cancer therapy: Exosomes and ferritin. Pharmacol Res. 2016;110:1-9.

13. Fan K, et al. Bioengineered ferritin nanoprobes for cancer theranostics. Handbook of Nanomaterials for Cancer Theranostics. 2018;143-175.

14. Kwon KC, et al. Enhanced *in vivo* tumor detection by active tumor cell targeting using multiple tumor receptor-binding peptides presented on genetically engineered human ferritin nanoparticles. Small. 2016;12:4241-4253.

15. Balaratnam S, et al. A piRNA utilizes HILI and HIWI2 mediated pathway to down-regulate ferritin heavy chain 1 mRNA in human somatic cells. Nucleic Acids Res. 2018; 46:10635-10648.

16. Marianna TR, et al. Ferritin is secreted *via* 2 distinct nonclassical vesicular pathways, Blood. 2018;131:342-352.

17. Zhengjie H, et al. Serum ferritin is a good indicator for predicting the efficacy of adult HLH induction therapy. Ann Med. (2022) 54: 283-292.

18. Jing P, et al. Ferritin-nanocaged ATP traverses the blood-testis barrier and enhances sperm motility in an asthenozoospermia model, ACS Nano. 2022;16: 4175–4185.

19. Wang B, et al. Targeted delivery of a STING agonist to brain tumors using bioengineered protein nanoparticles for enhanced immunotherapy. Bioact Mater.2022;16:232-248.

20. Wang Z, et al. Re-engineering the inner surface of ferritin nanocage enables dual drug payloads for synergistic tumor therapy. Theranostics. 2022;12:1800-1815.

21. Xinghan Wu, et al. Co-loaded lapatinib/PAB by ferritin nanoparticles eliminated ECM-detached cluster cells *via* modulating EGFR in triple-negative breast cancer. Cell Death Dis. 2022;13:557.

22. Zhang B, et al. Constructing a nanocage-based universal carrier for delivering TLR-activating nucleic acids to enhance antitumor immunotherapy. Nano Today.2022;46:101564.

23. Ren E, et al. Harnessing bifunctional ferritin with kartogenin loading for mesenchymal stem cell capture and enhancing chondrogenesis in cartilage regeneration. Adv Healthc Mater. 2022;11: e2101715.

24. Zhang X, et al. Biomimetic design of artificial hybrid nanocells for boosted vascular regeneration in ischemic tissues. Adv Mater. 2022;34:e2110352.

25. Xindong W, et al. A class of biocompatible dye-protein complex optical nanoprobes. ACS Nano. 2021;16:328–339.

26. Lu C, et al. Design of a gold clustering site in an engineered apo-ferritin cage. Commun Chem. 2022;5:39-41.

27. Dickey LF, et al. Differences in the regulation of messenger RNA for housekeeping and specialized-cell ferritin. A comparison of three distinct ferritin complementary DNAs, the corresponding subunits, and identification of the first processed in amphibia. J Biol Chem. 1987;262:7901-7907.

28. Ebrahimi KH, et al. A novel mechanism of iron-core formation by *Pyrococcus furiosus* archaeoferritin, a member of an uncharacterized branch of the ferritin-like superfamily. J Biol Inorg Chem. 2012;17:975-985.

29. Grant R, et al. The crytal structure of Dps, a ferritin homolog that binds and protects DNA. Nat Struct Biol. 1998;5:294-303.

30. Arnold A, et al. Characterization of the DNA-mediated oxidation of Dps, A bacterial ferritin. J Am Chem Soc. 2016;138:11290-11298.

31. Johnson E, et al. Crystal structures of a tetrahedral open pore ferritin from the hyperthermophilic archaeon *Archaeoglobus fulgidus*. Structure. 2005;13:637-648.

32. Sato Z, et al. Ferritin Assembly Revisited: A time-resolved small-angle x-ray scattering study. Biochemistry. 2016;55:287-293.

33. Kim M, et al. pH-dependent structures of ferritin and apoferritin in solution: Disassembly and reassembly. Biomacromolecules. 2011;12:1629-1640.

34. Maity B, et al. Single-molecule level dynamic observation of disassembly of the apo-ferritin cage in solution. Phys Chem Chem Phys. 2020;22: 18562-18572.

35. Li Z, et al. Importance of the subunit-subunit interface in ferritin disassembly: A molecular dynamics study. Langmuir. 2022;38:1106-1113.

36. Mehlenbacher M, et al. Iron oxidation and core formation in recombinant heteropolymeric human ferritins. Biochemistry. 2017;56:3900-3912.

37. Carmona F, et al. Study of ferritin self-assembly and heteropolymer formation by the use of Fluorescence Resonance Energy Transfer (FRET) technology. Biochim Biophys Acta Gen Subj. 2017;1861:522-532.

38. Koralewski M, et al. Morphology and magnetic structure of the ferritin core during iron loading and release by magnetooptical and NMR methods. ACS Appl Mater Interfaces. 2018;10:7777-7787.

39. Narayanan S, et al. On the structure and chemistry of iron oxide cores in human heart and human spleen ferritins using graphene liquid cell electron microscopy. Nanoscale. 2019;11:16868-16878.

40. Houben L, et al. A mechanism of ferritin crystallization revealed by cryo-STEM tomography. Nature. 2020;579:540-543.

41. Narayanan S, et al. Transmission electron microscopy of the iron oxide core in ferritin proteins: Current status and future directions. J of Phys D. 2019;52:453001.

42. Deng J, et al. Purification and characterization of new phytoferritin from black bean (*Phaseolus vulgaris L.*) seed. J Biochem. 2010;147:679-688.

43. Masuda T. Soybean ferritin forms an iron-containing oligomer in tofu even after heat treatment. J Agric Food Chem. 2015;63:8890-8895.

44. Yang R, et al. The interaction of DNA with phytoferritin during iron oxidation. Food Chem. 2014;153:292-297.

45. He D, et al. Ferritin family proteins and their use in bionanotechnology. N Biotechnol. 2015;32:651-657.

46. Pullin J, et al. Electron transfer from haem to the di-iron ferroxidase centre in bacterioferritin. Angew Chem Int Ed.2021;60:8376-8379.

47. Mohanty A, et al. Alteration of coaxial heme ligands reveals the role of heme in bacterioferritin from *Mycobacterium tuberculosis*. Inorg Chem. 2021;60:16937-16952.

48. Chiancone E, et al. The multifaceted capacity of Dps proteins to combat bacterial stress conditions: Detoxification of iron and hydrogen peroxide and DNA binding. Biochim Biophys Acta. 2010;1800:798-805.

49. Eren E, et al. Structural characterization of the *Myxococcus xanthus encapsulin* and ferritin-like cargo system gives insight into its iron storage mechanism. Structure. 2022;30:551-563.

50. Ross J, et al. Pore dynamics and asymmetric cargo loading in an encapsulin nanocompartment. Sci Adv. 2022;8:4461.

51. Turris V, et al. Humanized archaeal ferritin as a tool for cell targeted delivery. Nanoscale. 2017;9:647-655.

52. Macone A, et al. Ferritin nanovehicle for targeted delivery of cytochrome C to cancer cells. Sci Rep. 2019;9:11749.

53. Zhang S, et al. The size flexibility of ferritin nanocage opens a new way to prepare nanomaterials. Small. 2017;13.

54. Chen H, et al. Compartmentalized chitooligosaccharide/ferritin particles for controlled co-encapsulation of curcumin and rutin. Carbohydr Polym. 2022;290:119484.

55. Liang M, et al. H-ferritin-nanocaged doxorubicin nanoparticles specifically target and kill tumors with a single-dose injection. Proc Natl Acad Sci USA. 2014;111:14900-14905.

56. Bellini M, et al. Protein nanocages for self-triggered nuclear delivery of DNA-targeted chemotherapeutics in Cancer Cells. J Control Release.2014;196:184-196.

57. Inoue I, et al. One-step construction of ferritin encapsulation drugs for cancer chemotherapy, Nanoscale. 2021;13:1875-1883.

58. Bradley J, et al. Protein encapsulation within the internal cavity of a bacterioferritin. Nanoscale. 2022;14:12322-12331.

59. Tetter S, et al. Enzyme encapsulation by a ferritin cage. Angew Chem Int Ed. 2017;56:14933-14936.

60. Bulos J, et al. Design of a superpositively charged enzyme: Human carbonic anhydrase ii variant with ferritin encapsulation and immobilization. Biochemistry. 2021;60:3596-3609.

61. Shan H, et al. Targeted ferritin nanoparticle encapsulating CpG oligodeoxynucleotides induces tumor-associated macrophage M2 phenotype polarization into M1 phenotype and inhibits tumor growth. Nanoscale. 2020;12:22268-22280.

62. Kim H, et al. Ferritin nanocage-based methyltransferase SETD6 for COVID-19 therapy. Adv Funct Mater. 2020;30.

63. Lee E, et al. Nanocage-therapeutics prevailing phagocytosis and immunogenic cell death awakens immunity against cancer. Adv Mater. 2018;30.

64. Kang Y, et al. Rapid development of SARS-CoV-2 spike protein receptor-binding domain self-assembled nanoparticle vaccine candidates, ACS Nano. 2021;15:2738-2752.

65. Ahn B, et al. Four-fold channel-nicked human ferritin nanocages for active drug loading and pH-responsive drug release, Angew Chem Int Ed. 2018;57:2909-2913.

66. Zang J, et al. Ferritin cage for encapsulation and delivery of bioactive nutrients: From structure, property to applications. Crit Rev Food Sci Nutr. 2017;57:3673-3683.

67. Wang Z, et al. Bioengineered dual-targeting protein nanocage for stereoscopically loading of synergistic hydrophilic/hydrophobic drugs to enhance anticancer efficacy. Adv Funct Mater. 2021;31.

68. Jeon I, et al. Anticancer nanocage platforms for combined immunotherapy designed to harness immune checkpoints and deliver anticancer drugs. Biomaterials. 2021;270:120685.

69. Chen S, et al. Chaotrope-controlled fabrication of ferritin-salvianolic acid b- epigallocatechin gallate three-layer nanoparticle by the flexibility of ferritin channels. J Agric Food Chem. 2021;69:12314-12322.

70. Meng B, et al. Double-interface binding of two bioactive compounds with cage-like ferritin. J Agric Food Chem. 2020;68:7779-7788.

71. Moglia I, et al. Silver nanoparticle synthesis in human ferritin by photochemical reduction. J Inorg Biochem. 2020;206:111016.

72. Tchaikovsky A, et al. Quantification of ferritin-bound iron in murine samples for Alzheimer's disease studies using species-specific isotope dilution mass spectrometry. Metrologia. 2020;57.

73. Sen S, et al. Protein-nanoparticle complex structure determination by cryo-electron microscopy. ACS Appl Bio Mater. 2022.

74. Zhang Y, et al. Biomimetic design of mitochondria-targeted hybrid nanozymes as superoxide scavengers. Adv Mater. 2021;33:e2006570.

75. Zhang Y, et al. Nanocage-based capture-detection system for the clinical diagnosis of autoimmune disease. Small. 2021;17:e2101655.

76. Adams J, et al. Cardiac troponin I. A marker with high specificity for cardiac injury. Circulation. 1993;88:101-106.

77. Men D, et al. Self-assembly of ferritin nanoparticles into an enzyme nanocomposite with tunable size for ultrasensitive immunoassay. Acs Nano. 2015;9:10852-10860.

78. Akanda R, et al. Ferritin-triggered redox cycling for highly sensitive electrochemical immunosensing of protein. Anal Chem. 2018;90:8028-8034.

79. Yang L, et al. PEGylation improved electrochemiluminescence supramolecular assembly of iridium (iii) complexes in apoferritin for immunoassays using 2D/2D MXene/TiO$_2$ hybrids as signal amplifiers. Anal Chem. 2021;93:16906-16914.

80. Du Y, et al. Endoscopic molecular imaging of early gastric cancer using fluorescently labeled human H-ferritin nanoparticle. Nanomedicine. 2018;14:2259-2270.

81. Du Y, et al. Endoscopic molecular imaging of early gastric cancer using human heavy-chain ferritin nanaoparobe under confocal laser endomicroscopy. Gastrointest Endosc. 2018;87:AB169-AB170.

82. Truffi M, et al. Ferritin nanocages: A biological platform for drug delivery, imaging and theranostics in cancer. Pharmacol Res. 2016;107:57-65.

83. Wang Z, et al. Functional ferritin nanoparticles for biomedical applications, Front Chem Sci Eng. 2017;11:633-646.

84. Bellini M, et al. Engineered ferritin nanoparticles for the bioluminescence tracking of nanodrug delivery in cancer. Small. 2020;16:e2001450.

85. Liang M, et al. Bioengineered H-Ferritin nanocages for quantitative imaging of vulnerable plaques in atherosclerosis. ACS Nano. 2018;12: 9300-9308.

86. Liu M, et al. Hemin-Caged ferritin acting as a peroxidase-like nanozyme for the selective detection of tumor cells. Inorg Chem. 2021;60:14515-14519.

87. Tullio C, et al. Development of an effective tumor-targeted contrast agent for magnetic resonance imaging based on Mn/H-Ferritin nanocomplexes, ACS Appl Bio Mater. 2021;4:7800-7810.

88. Lin X, et al. Chimeric ferritin nanocages for multiple function loading and multimodal imaging. Nano Lett. 2011;11:814-819.

89. Jiang B, et al. Ferritin nanocages for early theranostics of tumors *via* inflammation-enhanced active targeting. Sci China Life Sci. 2021;65:328-340.

90. Fan K, et al. Magnetoferritin nanoparticles for targeting and visualizing tumour tissues. Nat Nanotechnol. 2012;7:459-464.

91. Jiang B, et al. GRP78-targeted ferritin nanocaged ultra-high dose of doxorubicin for hepatocellular carcinoma therapy. Theranostics. 2019;9:2167-2182.

92. Ma Y, et al. Tumor-penetrating peptide-functionalized ferritin enhances antitumor activity of paclitaxel. ACS Appl Bio Mater. 2021;4:2654-2663.

93. Dong Y, et al. ERK-peptide-inhibitor-modified ferritin enhanced the therapeutic effects of paclitaxel in cancer cells and spheroids. Mol Pharm. 2021;18:3365-3377.

94. Zuo T, et al. pH-Sensitive molecular-switch-containing polymer nanoparticle for breast cancer therapy with ferritinophagy-cascade ferroptosis and tumor immune activation. Adv Healthc Mater. 2021; 10:e2100683.

95. Cai Y, et al. use of ferritin capped mesoporous silica nanoparticles for redox and pH triggered drug release *in vitro* and *in vivo*. Adv Funct Mater. 2020;30:2002043.

96. Lee E, et al. Engineered proteinticles for targeted delivery of sirna to cancer cells. Adv Funct Mater. 2015;25:1279-1286.

97. Li L, et al. Ferritin-mediated siRNA delivery and gene silencing in human tumor and primary cells. Biomaterials. 2016;98:143-151.

98. Pediconi N, et al. Design and synthesis of piperazine-based compounds conjugated to humanized ferritin as delivery system of sirna in cancer cells. Bioconjug Chem. 2021;32:1105-1116.

99. Palombarini F, et al. Self-assembling ferritin-dendrimer nanoparticles for targeted delivery of nucleic acids to myeloid leukemia cells. J Nanobiotechnology. 2021;19:172.

100. Huang H, et al. Ca$(2+)$ participating self-assembly of an apoferritin nanostructure for nucleic acid drug delivery. Nanoscale. 2020;12:7347-7357.

101. Huang H, et al. Genetic recombination of poly (l-lysine) functionalized apoferritin nanocages that resemble viral capsid nanometer-sized platforms for gene therapy. Biomater Sci. 2020;8:1759-1770.

102. Pan X, et al. One-in-one individual package and delivery of CRISPR/Cas9 ribonucleoprotein using apoferritin. J Control Release. 2021;337:686-697.

103. Pan X, et al. Tetralysine modified H-chain apoferritin mediated nucleus delivery of chemotherapy drugs synchronized with passive diffusion. J Drug Deliv Sci Technol. 2021;61:102132.[Crossref] [Google Scholar]

104. Liu Z, et al. A novel method for synthetic vaccine construction based on protein assembly. Sci Rep. 2014;4:7266.

105. Qu Y, et al. Stability of Engineered Ferritin Nanovaccines Investigated by Combined Molecular Simulation and Experiments. J Phys Chem B.2021;125:3830-3842.

106. Houser KV, et al. Team VRCS, Safety and immunogenicity of a ferritin nanoparticle H2 influenza vaccine in healthy adults: A phase 1 trial. Nat Med. 2022;28:383-391.

107. Han JA, et al. Ferritin protein cage nanoparticles as versatile antigen delivery nanoplatforms for dendritic cell (DC)-based vaccine development. Nanomedicine. 2014;10:561-569.

108. Joyce MG, et al. SARS-CoV-2 ferritin nanoparticle vaccines elicit broad SARS coronavirus immunogenicity. Cell Rep. 2021;37:110143.

109. King HAD, et al. Efficacy and breadth of adjuvanted SARS-CoV-2 receptor-binding domain nanoparticle vaccine in macaques. Proc Natl Acad Sci. 2021;118.

110. Joyce MG, et al. A SARS-CoV-2 ferritin nanoparticle vaccine elicits protective immune responses in nonhuman primates. Sci Transl Med. 2022;14.

111. Wang W, et al. Ferritin nanoparticle-based SpyTag/SpyCatcher-enabled click vaccine for tumor immunotherapy. Nanomedicine. 2019;16:69-78.

112. Ma X, et al. Nanoparticle vaccines based on the Receptor Binding Domain (RBD) and Heptad Repeat (HR) of SARS-CoV-2 elicit robust protective immune responses. Immunity. 2020;53:1315-1330.

113. Li Y, Split-inteins and their bioapplications. Biotechnol Lett. 2015;37:2121-2137.

114. Tang S, et al. Versatile functionalization of ferritin nanoparticles by intein-mediated trans-splicing for antigen/adjuvant co-delivery. Nano Lett. 2019;19:5469-5475.

115. Balakrishnan PB, et al. Exploiting unique alignment of cobalt ferrite nanoparticles, mild hyperthermia, and controlled intrinsic cobalt toxicity for cancer therapy. Adv Mater. 2020;32:22-29 .

116. Xu H, et al. Experimental evaluation on the heating efficiency of magnetoferritin nanoparticles in an alternating magnetic field. Nanomaterials. 2019;9:1457.

117. Fantechi E, et al. A smart platform for hyperthermia application in cancer treatment: Cobalt-doped ferrite nanoparticles mineralized in human ferritin cages. ACS Nano. 2014;8:4705-4719.

118.   Min X, et al. AIE nanodots scaffolded by mini-ferritin protein for cellular imaging and photodynamic therapy. Nanoscale. 2020; 12:2340-2344.

119.   Zhen Z, et al. Protein nanocage mediated fibroblast-activation protein targeted photoimmunotherapy to enhance cytotoxic t cell infiltration and tumor control. Nano Lett. 2017;17:862-869.

120.   Zhou SY, et al. FAP-Targeted photodynamic therapy mediated by ferritin nanoparticles elicits an immune response against cancer cells and cancer associated fibroblasts. Adv Funct Mater. 2021;31:ARTN 2007017.

121.   Liu M, et al. Nanobody-Ferritin conjugate for targeted photodynamic therapy. Chemistry. 2020;26:7442-7450.

122.   Zhu Y, et al. Oxygen self-supply engineering-ferritin for the relief of hypoxia in tumors and the enhancement of photodynamic therapy efficacy. Small. 2022;18:e2200116.

123.   Medzhitov R, Origin and physiological roles of inflammation. Nature. 2008; 454:428-435.

124.   Lee W, et al. A Double-chambered protein nanocage loaded with thrombin receptor agonist peptide (trap) and gamma-carboxyglutamic acid of protein c (PC-Gla) for sepsis treatment. Adv Mater. 2015;27:6637-6643.

125.   Sontz PA, et al. A metal organic framework with spherical protein nodes: Rational chemical design of 3d protein crystals. J Am Chem Soc. 2015;137:11598-11601.

126.   Zheng B, et al. Designed two- and three-dimensional protein nanocage networks driven by hydrophobic interactions contributed by amyloidogenic motifs. Nano Lett. 2019;19:4023-4028.

127.   Yang R, et al. Self-assembly of ferritin nanocages into linear chains induced by poly (alpha, L-lysine). Chem Commun. 2014;50:481-483.

128.   Liu Q, et al. Modular assembly of tumor-penetrating and oligomeric nanozyme based on intrinsically self-assembling protein nanocages. Adv Mater. 2021; 33:e2103128.

129.   Edwardson TGW, et al. Virus-inspired function in engineered protein cages. J Am Chem Soc. 2019;141:9432-9443.

130.   Beck T, et al. Construction of Matryoshka-type structures from supercharged protein nanocages. Angew Chem Int Ed. 2015;54:937-940.

131.   Bailey JB, et al. Tunable and cooperative thermomechanical properties of Protein-Metal-Organic frameworks. J Am Chem Soc. 2020;142:17265-17270.